AN ABSTRACT OF THE THESIS OF

Elizabeth M. Polsdofer for the degree of Master of Science in Medical Physics presented on May 19, 2016

Title: Testing Continuity between Versions 5.3.9 and 6.3.1 of Plaque Simulator for Planning Eye Plaque Brachytherapy Cases

Abstract Approved:

Richard J. Crilly

The purpose of this study is to examine the challenges of accepting and commissioning a new treatment planning system for eye plaque brachytherapy. Currently Oregon Health and Science University (OHSU) utilizes v5.3.9 of the Plaque Simulator software to plan all of its eye plaque brachytherapy cases. However, v5.3.9 is no longer supported by its manufacturer, Eye Physics, LLC. OHSU is upgrading to a supported version of Plaque Simulator, v6.3.1. Prior to planning brachytherapy cases in v6.3.1 an investigation needs to be launched concerning the technical and dosimetric differences between v5.3.9 and v6.3.1.

A study investigating the percent difference in doses to the prescription point, sclera, and tumor apex between v5.3.9 and v6.3.1 was created for 28 patients who had undergone eye plaque brachytherapy during 2015 and 2016 at OHSU. The sample size was distributed evenly across five out of seven of the Collaborative Ocular Melanoma Study (COMS) non–notched plaques (n=5 for each plaque size) with a smaller sample size for the notched COMS 20 plaque (n=3). Doses to the prescription point, sclera, and tumor apex were compared to treatment plans created in v5.3.9 and v6.3.1. Acceptance of v6.3.1 requires that the percent difference between its results and v5.3.9 are less than 5%.

The prescription point percent differences between v5.3.9 and v6.3.1 were 0% for all (28 out of 28) cases. The sclera doses were between 2–4% lower in v6.3.1 than v5.3.9 for 93% (26 out of 28) cases; the remaining two cases (Trials 24 and 26) had percent differences of –5.21% and –6.22%, respectively. The tumor apex percent differences were less than 1% for 89% (25 out of 28) of cases and less than 1.5% for the remaining three cases. Dosimetric differences between v5.3.9 and v6.3.1 are attributed to the change in the carrier factor correction data set used to calculate the attenuation of radiation via the Silastic insert of the COMS plaque. The percent differences for carrier factor correction between the outer (r=2 mm) and inner (r=3 mm) sclera are –3.36% and –1.82%, respectively. The carrier factor corrections in v6.3.1 are from *Chiu Tsao et al.*

1993 for I–125 seed model 6711. It is recommended that the data set from *Chiu Tsao et al. 1993* be adopted until a more suitable data set is found.

The effect of planning cases based on the true location of the tumor within the eye (3D planning) versus planning to the apex of the tumor (1D planning) were examined in v6.3.1. The same patient data was used as in the comparison between v5.3.9 and v6.3.1, but the tumors locations were moved. A best guess was made as to the location of the tumor based on physician notes and fundus images. The purpose of this study was to establish proof of concept.

The doses to the prescription point remained unchanged for 1D versus 3D planning. Doses to the sclera were unchanged for 75% (21 out of 28) of cases. Of the cases where dose changed between 1D and 3D planning, the percent difference was no greater than 0.06% to the sclera. Doses to the tumor apex remained unchanged for 93% (26 out of 28) cases. The cases that saw a change in tumor apex only saw a percent difference of 0.1% and 0.01%, respectively. Doses to the prescription point, sclera, and tumor apex are negligible and do not affect the quality of care. Although 3D planning requires an additional time commitment from the physicist or dosimetrist, proof of concept has been established and is recommended for estimating normal tissue doses.

Testing Continuity between Versions 5.3.9 and 6.3.1 of Plaque Simulator for Planning Eye Plaque Brachytherapy Cases

by
Elizabeth M. Polsdofer

A THESIS

submitted to

Oregon State University

in partial fulfillment of
the requirements for the
degree of

Master of Science

Presented May 19, 2016
Commencement June 2017

Master of Science thesis of Elizabeth M. Polsdofer presented on May 19, 2016.

APPROVED:

Major Professor, representing Medical Physics

Head of the School of Nuclear Science and Engineering

Dean of the Graduate School

In understand that my thesis will become part of the permanent collection of Oregon State University libraries. My signature below authorizes release of my thesis to any reader upon request.

Elizabeth M. Polsdofer, Author

ACKNOWLEDGMENTS

I want to acknowledge the faculty and staff at Oregon State and Oregon Health and Science University for my graduate education and for answering each of my questions with patience. I enjoyed connecting and learning from each one of you how to be a better clinician and physicist.

In particular, a big thank you to my thesis advisor, Richard Crilly, for supporting me in my research endeavors. Thank you for advising me to not take on several other side projects and helping me with the additional research that I did take on.

To the staff at the Casey Eye Institute who let me observe numerous eye plaque procedures. In particular, Alison Skalet for welcoming me into her OR. A big thank you to Marika Yumang and Philip Turner who taught me the finer points of reading echosonography images.

I would like to thank Alyssa Miller, for her love and support throughout the years. I hope you physics; you're my person.

Finally, to the Iowa State Daily and Iowa State's Greenlee School of Journalism and Communication for teaching me how to write under the pressure of a deadline. This thesis is "ready for copyeditor."

TABLE OF CONTENTS

LIST OF FIGURES

LIST OF TABLES

1. Introduction

Ocular melanoma is the most common form of intraocular cancer with 2500 new cases presenting annually in the United States.[1] Intraocular tumors are difficult to resect and are often treated with radiation or removal of the eye, enucleation. The role of radiation in treating ocular melanomas has grown. As a result the number of seed and plaque models to accomodate these types of tumors has also grown. With the increased frequency of eye plaque brachytherapy to treat intraocular tumors the field has seen an urgent need to create more accurate methods for calculating radiation transport to the tumor and through normal tissues.

The human eye is 25 mm–30 mm in diameter.[2] It is the organ responsible for vision and thus has a high impact on the patient's quality of life. Prior to eye plaque brachytherapy the standard of care for ocular melanomas was a resection of the eye. However, enucleation leads to definitive vision loss and the cosmetic loss of the eye. A desire to preserve vision and retain one's eye is a compelling reason why some patients with small and medium ocular tumors elect to undergo eye plaque brachytherapy.

Eye plaque brachytherapy is a form of low dose rate (LDR) brachytherapy. LDR brachytherapy is any radionuclide those dose delivers 0.4–2 Gy/hr over the course of treatment. Medium dose rate (MDR) sources deliver doses at a rate of 2–12 Gy/hr. High dose rate (HDR) sources have dose rates greater than 12 Gy/hr and are used at OSHU to treat gynecological cancers. LDR brachytherapy is used to treat prostate, breast, and intraocular tumors and may be either temporary or permanent implants.

The two radionuclides of interest for LDR brachytherapy in eye plaque brachytherapy are Iodine–125 (I–125) and Palladium–103 (Pd–103). Iodine–125 has a half-life of 59.4 days and an average energy of 28.5 keV per gamma–ray. Palladium–103 has a half–life of 17 days and an average energy of 20.8 keV. Of the two radionuclides, I–125 is used to treat intraocular tumors at OHSU.

The growth in eye plaque brachytherapy led to the formation of the Collaborative Ocular Melanoma Study (COMS) in 1985 to standardize the quality of care for this procedure. In order to test the effectivity of eye plaque brachytherapy, COMS conducted two prospective randomized clinical trials with large and medium sized tumors, respectively.[3]

The first COMS clinical trial used a stereotactic body radiation therapy (SBRT)–

like fractionation scheme of 4 Gy/fx in 5 daily fractions for a total of 20 Gy.[4] The patients selected for this trial had tumors with an apical height of 10 mm or greater or a maximal tumor basal dimension of 16 mm or greater. The experimental group received this radiation prior to enucleation and the control group did not. Both groups underwent enucleation and were followed up. Irradiating the patients prior to enucleation did not appear to offer any long term survival benefits over enucleation without radiation.

The second COMS clinical trial tested 100 Gy of Iodine–125 seeds versus enucleation for medium size tumors.[5] Patients selected for this clinical trial had tumors with apical heights between 2.5 and 10 mm with a maximal tumor basal dimension equal to or less than 16 mm. No significant differences in long term survival presented itself between the two groups, establishing the effectiveness of brachytherapy in treating medium–sized ocular melanomas.

Once the effectiveness of eye plaque brachytherapy to treat ocular melanomas was demonstrated the need to establish a standard for calculating doses to the prescription point was expressed. Traditionally, doses to the prescription point and normal tissues have been calculated with point–source approximations in an infinite water medium. However, there are several significant inhomogeneities present due to the low energy nature of I–125 and Pd–103 that have seed energies less than 30 keV.

At low energies the photoelectric effect dominates over Compton scatter, especially for high atomic number (Z) objects. The gold–alloy COMS plaque, trade name Modulay, has a high Z (Z=79 for gold) that attenuates photons as well as the Silastic insert ($Z_{eff} \sim 11$) that has a slightly higher Z than water and the surrounding tissues ($Z_{eff} \sim 7.4$).[6]

There is also a sharp dose fall off and important critical structures in the eye within millimeters of each other. Heterogeneities within the plaque material and eye itself makes accurately calculating doses to the tumor and critical structures challenging.

All eye plaque brachytherapy cases at Oregon Health and Science University (OHSU) are planned on version 5.3.9 (v5.3.9) of Plaque Simulator by Eye Physics, LLC. The tumor dimensions are taken from echosonograms of the lesion and modeled in Plaque Simulator. OHSU uses an IsoAid IAI–125U model seed and fully loads their plaques with seeds of uniform activity. The plaque size and style is ordered by the ophthalmologist and the prescription point and dose is given by the radiation oncologist.

The treatment plan is created with the tumor assumed to be in the default position in Plaque Simulator. The default tumor position is on the 9 o'clock hour with the tumor being centered on the equator. The plaque is placed directly over the tumor. A seed strength is calculated that places 85 Gy at the prescription point. The prescription point is determined by the radial length of the tumor. This method only works to calculate the dose across the tumor thickness and does not accurately calculate doses to normal

tissues.

Indeed, calculating doses to normal tissues is not currently a part of OHSU's protocol for planning eye plaque brachytherapy cases. OHSU creates treatment plans in Plaque Simulator based solely on covering the prescription point.

As per Task Group–129 (TG–129)'s suggestion a spreadsheet calculation is used to double check Plaque Simulator's treatment plan.[1] This is the extent of the current treatment planning process for eye plaque brachytherapy cases at OHSU.

However, v5.3.9 of Plaque Simulator is no longer supported and thus OHSU is upgrading to version 6.3.1 (v6.3.1).

The purpose of the thesis is to examine the dosimetric and interface differences between v5.3.9 and v6.3.1. Protocols for calculating doses to the prescription point and normal tissues are constantly updating and evolving. With each new update in protocol and treatment planning systems there is a subsequent need to discuss what changes have been made and how these changes will affect the quality of care delivered to patients. The goal of this document is to facilitate a discussion regarding the use of v6.3.1 and how the treatment planning process can be improved to provide better dose estimates to normal tissues.

2. Description and history of eye plaque brachytherapy

As the field advances the medical physics community has the advantage and disadvantage of having a plethora of literature about the dosimetry of brachytherapy sources from Monte Carlo simulations and measured data for a variety of seed models and manufacturers. However, this information is double–edge sword as some clinics will adapt one set of data while another clinic will make calculations based off another study.

Task Group–43 (TG–43)[7] set down a standard dose calculation formalism for brachytherapy sources and established the need for consensus data for consistent medical practices in the field across all clinics. Universal adaption of the consensus data allows research groups to compare their data to each other without having to make several corrections for using different data sets.

The TG–43 dose calculation formalism and consensus data has been revisited twice with an update (TG–43U1) by *Rivard et al. 2004* [8] and a supplement to the update (TG–43U1S1) by *Rivard et al. 2007*.[9] The TG–43 dose calculation formalism was slightly modified in TG–43U1 and additional consensus data added. TG–43U1S1 addressed questions on the consensus data in TG–43U1 while adding consensus data from additional seed models and manufacturers. An overview of the TG–43 family and its dose calculation parameters is given in Section 2.1.

A description of the consensus data is listed in Section 2.2. with the relevant consensus data for the IsoAid IAI–125U seed. Only this seed model and manufacturer is shown since it is the only source used to plan and treat eye plaque brachytherapy cases at OHSU.

Finally, a brief overview of the recommendations given in TG–129 is discussed in Section 2.3.

2.1. Dose Calculations

Due to the small size of the eye and the proximity of critical structures within the eye, dosimetry for eye plaque brachytherapy presents unique challenges. In order to comprehensively compare studies to each other, COMS recommends a simplified method to calculate eye plaque brachytherapy dosimetry. The simplified method assumes a point–source approximation in an infinite homogeneous water medium with no corrections for

heterogeneities. Although these dose calculations are simple in nature they allow a standardization for comparing the results of future studies.

Recommendations to the dose calculations became more developed when the field moved toward a new primary standard of using air kerma strength. TG–43 gave an update to the simplified method recommended by COMS. Regardless of these updates, the COMS group recommends that physicists continue to use point–source approximations in water as the primary method to calculate the dosimetry for treatment plans.

2.1.1. Dose calculations prior to TG–43

Prior to TG–43 brachytherapy sources were calculated using the formalism described in Equation 2.1.

$$\dot{D}(r) = A_{app} f_{med} (\Gamma_\delta)_x (1/r^2) T(r) \bar{\Phi}_{an} \tag{2.1}$$

- Apparent activity, A_{app}
- Exposure–to–dose conversion factor, f_{med}
- Exposure rate constant, $(\Gamma_\delta)_x$
- Tissue attenuation factor, $T(r)$
- Anisotropy constant, Φ_{an}

The dosimetry for each source was not based on a standard set of consensus data, but calculated for each individual seed. This formalism was also created prior to the widespread adoption of the air kerma strength national calibration standards.

2.1.2. Task Group–43

The purpose of TG–43, published by *Nath et al. 1995*,[7] was to create a new formalism for calculating brachytherapy sources. Although not fully present in TG-43, *Nath et al. 1995* expressed the goal of publishing a set of a consensus data in the future for seed models and sources used for brachytherapy.

Consensus data will allow clinicians to compare brachytherapy protocols to each. Prior to TG–43 the dosimetry of brachytherapy sources was based on the clinic using the source. By standardizing brachtherapy dosimetry methods the field will able to create more consistent dose calculations and provide comparable quality of care across the country regardless of clinical protocols and seed manufacturers. The first step in producing consensus data is standardizing how dose is calculated.

Dose calculation formalism

The formalism for TG–43 is different from previous formalism (see Equation 2.1) in that the TG–43 formalism tries to separate out interrelated quantities into several different terms. Pre–TG–43 formalism estimated assumed a point–source geometry, used exposure rate constants, tissue attenuation factors, tissue equivalent phantoms, no scattering medium, and assumed isotropy.

TG–43 formalism (see Equation 2.2) calculates dosimetry using air kerma strength, a geometry factor, radial dose factor, and an anisotrophy function.

$$\dot{D}(r,\theta) = S_K \Lambda \left[\frac{G(r,\theta)}{G(r_0,\theta_0)}\right] g(r) F(r,\theta) \tag{2.2}$$

- Air kerma strength, S_K
- Dose rate constant, Λ
- Geometry factor, $G(r,\theta)$
- Radial dose function, $g(r)$
- Anisotropy function, $F(r,\theta)$

Reference point

The reference point for TG–43's formalism, as listed in Equation 2.2, is at 1 cm along the transverse axis of the long axis of the seed.[7] This position corresponds to 90° in the viewer's frame of reference with the distal ends of the seeds at 0° and 180°. The origin of the frame is at the seed's center.

Air kerma strength, S_K

Air kerma strength, S_K, is the rate of air kerma at a point along the transverse axis (perpendicular to the long axis of the seed) at a distance of one meter away from the source in free space.[7] The air kerma strength term takes into account photons of all energy and is defined by Equation 2.3.

$$S_K = \dot{K}(d) d^2 \tag{2.3}$$

- Air kerma rate in free space, $K(d)$
- Calibration distance, d

At a distance of one meter away from the seed, which is linear in nature, it is safe to treat the seed as a point–source. These measurements are performed in air with corrections for air attenuation.

Plaque Simulator calculates sources that have sufficient activity to treat the prescription point. The physicist will order seeds with an apparent activity sufficient to treat the patient within ±5% of the prescribed dose to the tumor.

When the seeds are delivered to the clinic the physicist will measure the exposure rate of the source in a Well chamber. The Well chamber is a ionization chamber whose response is dependent on the source position within the detector and the length of source.

It should be noted that seed models from different manufactures will have a design unique to their model. Therefore the physicist should note which calibration factor to use as the variance in seed construction will affect the way radiation travels from the radioactive source to the target volume. These differences in seed design also result in differences in absorption effects in the seed shell.

Once the correct calibration factor is selected then an accurate measurement of the seed's exposure rate can be made. The ion chamber collects the ion pairs created when photons from the source ionize the air molecules within the chamber. The greater the activity of the source the more ion pairs are created. Exposure specifically measures the electrons created in the ion pair.

A disadvantage of Well chambers is that they are dependent on the energy of the source. Some photons from the radionuclide will be attenuated in the shell of seed, causing a shift in the energy spectrum and reducing the number of photons to be measured in the Well chamber. The Well chamber should have a calibration traceable to a standard national laboratory.

Dose rate constant, Λ

The dose rate constant, Λ, is the dose to rate at a distance of 1 cm from the origin of the source along the transverse axis. The dose rate constant is an absolute quantity that depends on the air kerma strength of the source.

The dose rate constant converts from measurements in air to measurements in water.

Geometry factor, $G(r, \theta)$

The geometry factor takes into account the shape of the source. The source's shape will affect how it distributes radiation in a medium. At far enough distances all seeds can be treated as point–sources, but small distances require treating the seeds as line sources. The relationship between the geometry factor and the distance from the source, source length, and angle of the source is listed in Equations 2.4 and 2.5 for point– and line–sources, respectively.

$$G(r, \theta) = r^{-2}, \quad \text{if point–source} \tag{2.4}$$

- Radial distance from source, r

$$G(r,\theta) = \begin{cases} \frac{\beta}{Lrsin\theta}, & \text{if } \theta \neq 0^\circ \\ (r^2 - L^2/4)^{-1}, & \text{if } \theta = 0^\circ \end{cases} \tag{2.5}$$

- Distance from the source, center r
- Angle, in radians, between the closest part of the radioactive length to the point of calculation, β
- Length of the source, L
- Angle between the center of the source and the long axis of the source in relationship to the point of measurement, θ

The geometry factor does not take into account photon absorption and scattering. Photon absorption and scattering treated in the radial dose function, $g(r)$.

Radial dose function, $g(r)$

The radial dose function, $g(r)$ takes into account the effect of photon absorption and scattering on dose distribution. The radial dose function is only measured along the transverse axis, which is perpendicular to the long axis of the source. The radial dose function is relative to the reference point at an angle of 90° and a distance of 1 cm.

The full definition the radial dose function is listed in Equation 2.6 with the reference coordinates explicitly written out in Equation 2.7.

$$g(r) = \frac{\dot{D}(r,\theta_0)G(r_0,\theta_0)}{\dot{D}(r_0,\theta_0)G(r,\theta_0)} \tag{2.6}$$

$$g(r) = \frac{\dot{D}(r,90^\circ)G(1\text{ cm},90^\circ)}{\dot{D}(1\text{ cm},90^\circ)G(r,90^\circ)} \tag{2.7}$$

Anisotropy function, $F(r,q)$

The anisotropy function, $F(r,\theta)$, measures how differences in dose distribution surrounding the source vary with angle and distance. Anisotropy occurs in part because the seed is a line–source and not a point–source. Another reason for anisotropy is self–filtration, the attenuation caused by source photons having to pass through source material, of the radiation through the material surrounding the radioactive source and the source itself. The anisotropy takes into account photon absorption and scatter within the medium.

Equation 2.8 represents the anisotropy function.

$$F(r,\theta) = \frac{\dot{D}(r,\theta)G(r,\theta_0)}{\dot{D}(r,\theta_0)G(r,\theta)} \tag{2.8}$$

Measurements with TG–43 formalism

By separating out the different quantities clinicians are able to get a better dose estimate for a two–dimensional line source as opposed to a one–dimensional point source.

It is appropriate to treat the brachtherapy seed as a point source if measuring a more than 3 cm from the source. However, for eye plaque brachytherapy, where there are several normal tissues within millimeters of each other and the target is within millimeters of the source itself. Treating the seed as a point source will yield inadequate dosimetry for normal tissues proximal to the plaque as well as to the prescription point.

The data presented in TG–43 is based off doses to solid water that have been converted to doses in water. Basic dosimetric calculations approximate human tissues to water. While approximating humans to water is a reasonable gross dosimetric estimation the presence of heterogeneities will affect doses to critical structures.

TG–43 focused specifically on Iridium–192 (Ir–192), Iodine–125 (I–125), and Palladium–103 (Pd–103) sources for the use of low–dose rate (LDR) and high—dose rate (HDR) brachytherapy. Monte Carlo simulations were made for each source and compared to dosimetric measurements to solid water converted to liquid water. There was good agreement between the Monte Carlo and measured data for Ir–192 and I–125, but insufficient agreement for Pd–103.

Further data for Pd–103 was added with TG–43U1.

2.1.3. Task Group–43 Update

In 2004 *Rivard et al.* published an update to TG–43. The update was published due to the increasing large number of seed models available for the purpose of interstitial brachytherapy, updated standards in air–kerma strength, and because the literature on brachytherapy dosimetry had grown since the original 1995 publication of TG–43.

The differences between TG–43 and TG–43U1 are listed in verbatim in TG–43U1[8] as:

- A revised definition of air–kerma strength
- Elimination of *apparent activity* for specification of source strength
- Elimination of the anisotropy constant in favor of the distance–dependence one–dimensional anisotropy function
- Guidance on extrapolating tabulated TG–43 parameters to longer and shorter distances
- Correction for minor inconsistencies and omissions in the original protocol and its implementation

Unlike TG–43 that focused on both low– and high–dose rate brachytherapy sources,

TG–43U1 examines only low–dose rate sources. In particular TG–43U1 calculates the dose–rate distributions for certain I–125 and Pd–103 seed models. The dose–rate distributions of neutrons and beta particles are not addressed in TG–43U1.

Measurements of the dose–rate distributions of these sources were calculated primarily with LiF TLDs[10][11][12] and Monte Carlo simulations[10][13][14][15][16]. Several researchers created data sets based on their measurements. However, as more data became available for each source model it became a conundrum choosing which data set to use in calculating dose–rate distributions for brachytherapy sources. Thus, TG–43U1 thoroughly reviewed the literature and data sets for each seed model to come up with the consensus data.

The consensus data will allow future research studies to be comparative to each other by standardizing the parameters used to calculate dose by each model. Each model has its own set of dosimetric parameters because each seed model is designed differently in terms of shielding and radioactivity distribution.

The recommendations of TG–43U1 are for clinics to adopt its revised dose–calculation protocols and that the consensus data be used to calculate interstitial brachytherapy doses. The transition from TG–43 to TG–43U1 may result in some changes to patient tumor and normal tissues doses. Thus, it is recommended that a radiation oncologist is consulted prior to complete implementation of the TG–43U1 protocol.

Dose calculation for 2D formalism

The general 2D formalism for TG–43U1 (see Equation 2.9) is similar to the TG–43 formalism (see Equation 2.2).

$$\dot{D}(r,\theta) = S_K \Lambda \frac{G_L(r,\theta)}{G_L(r_0,\theta_0)} g_L(r) F(r,\theta) \tag{2.9}$$

- Air–kerma strength, S_K
- Dose–rate constant, Λ
- Geometry function, $G_L(r,\theta)$
- Radial dose function, $g_L(r)$
- 2D anisotropy function, $F(r,\theta)$

This formalism assumes that there is symmetry along the transverse axis with respect to the radioactive distribution of the source.

The terms within Equation 2.9 are further described in the following sections.

Reference point

The reference point for TG–43U1's 2D formalism is the same as for TG–43 (see Equation 2.2); at 1 cm along the transverse axis of the long axis of the seed. This position corresponds to 90° in the viewer's frame of reference with the distal ends of the seeds at 0° and 180°. The origin of the frame is at the seed's center.

Air–kerma strength, S_K

The definition for air–kerma strength, S_K, is similar to as stated in TG–43, but with an important difference. TG–43 defines air kerma strength, S_K, to include photons of all energies (see Equation 2.3). However TG–43U1 measurements air kerma strength from photons above a cutoff energy, δ (see Equation 2.10).

$$S_K = \dot{K}_\delta(d)d^2 \tag{2.10}$$

The cutoff energy, usually 5 keV, removes contaminate photons from the air–kerma strength measurement. The contaminate photons are usually a product of characteristic x–rays that originate within the shell of the brachytherapy source. These photons do not travel far in tissue, usually less than 0.1 cm, but will travel to the calibration distance of 1 m in air. By removing these contaminant photons a better estimate of the true dose–rate distribution will be measured, though dosimetry at small distances remains challenging.

Dose–rate constant, Λ

The dose–rate constant remains unchanged from its TG–43 definition and is defined by Equation 2.11

$$\Lambda = \frac{\dot{D}(r_0, \theta_0)}{S_K} \tag{2.11}$$

- Dose–rate at the reference point, $\dot{D}(r_0, \theta_0)$
- Air–kerma strength, S_K

The dose–rate constant depends on the radionuclide (I–125 vs. Pd–103) and what seed model is being used. The distribution of the radioactivity and seed design influences the dose–rate constant as well as the methodology used to calculate air–kerma strength.

Units for the dose–rate constant units are in $[cGyhr^{-1}U^{-1}]$. The purpose of the dose–rate constant is to convert measurements in air to measurements in water.

Geometry function, $G(r, \theta)$

The purpose of the geometry function, $G(r, \theta)$ is to take into account how the geometry of the radioactive part of the seed affects dose–rate distribution. Similar to TG–43, TG–43U1's geometry function does not consider photon scatter or attenuation throughout the medium. Calculating the geometry function using more appropriate or complex equations will result in a stronger interpolation value from the consensus data.

The equation for a point–source is the same as listed in TG–43 (see Equation 2.4), but with a subscript denoting that the source is a point (see Equation 2.12).

$$G_P(r, \theta) = r^{-2}, \quad \text{if point–source} \tag{2.12}$$

- Radial distance from source, r

A simple, point–source calculation assumes a pure inverse square law for dose–rate falloff from a source. However, the treatment of a point–source for 2D formalism is not recommended by TG–43U1. The formalism for a line–source is split into two parts that are dependent on angle from the source to point of measurement (see Equation 2.13).

$$G_L(r, \theta) = \begin{cases} \frac{\beta}{Lr sin\theta}, & \text{if } \theta \neq 0^\circ \\ (r^2 - L^2/4)^{-1}, & \text{if } \theta = 0^\circ \end{cases} \tag{2.13}$$

- Distance from the source, center r
- Angle, in radians, between the closest part of the radioactive length to the point of calculation, β
- Length of the source, L
- Angle between the center of the source and the long axis of the source in relationship to the point of measurement, θ

Like Equation 2.12, the TG–43U1 formalism has updated Equation 2.13 to include a subscript denoting that the source is a line–source.

Radial dose function, $g(r)$

The radial dose function for TG–43U1 (see Equation 2.14) is similar to the TG–43 formalism (see Equation 2.6), which the exception that TG–43U1 defines the function more broadly.

$$g_X(r) = \frac{\dot{D}(r, \theta_0)}{\dot{D}(r_0, \theta_0)} \frac{G_X(r_0, \theta_0)}{G_X(r, \theta_0)} \tag{2.14}$$

The subscript, X, denotes that Equation 2.14 applies to both a point– and line–source.

The radial dose function examines the photon scatter and attenuation that was previously not considered with the geometry factor.

In creating the consensus data linear interpolation was used between data points. However, TG–43U1 notes that some treatment planning systems use a fifth order polynomial fit as describe in Equation 2.15.

$$g_X(r) = a_0 + a_1 r + a_2 r^2 + a_3 r^3 + a_4 r^4 + a_5 r^5 \tag{2.15}$$

2D anisotrophy function

The TG–43U1 formalism for the anisotrophy function (see Equation 2.16) is the same as for TG–43 (see Equation 2.8), aside from the subscript L reflecting the updated formalism for the geometry function.

$$F(r,\theta) = \frac{\dot{D}(r,\theta)}{\dot{D}(r,\theta_0)} \frac{G_L(r,\theta_0)}{G_L(r,\theta)} \tag{2.16}$$

The anisotropy function measures how much the dose–rate changes based on the relative polar angle of the point of measurement. A separate equation is created for the anisotropy function for 1D formalism. However, given the importance of calculating dosimetry at a small distances for eye plaque brachytherapy, a discussion of the 1D anisotropy function is not given.

2.1.4. Supplement to the Task Group–43 Update

The purpose of the supplement to the Task Group–43 Update[9] is to address questions that arose about the consensus data and brachytherapy dosimetry methodology. In particular, the need for a supplement to the update arose from an increase in the number of vendors and models of brachytherapy seeds.

Each seed model and manufacturer may have a different design and activity distribution within the seed. Therefore, it is appropriate to create consensus data for each of the seed models. The additional seed models addressed in TG–43U1S1 are:

- I–125
  - Amersham model 6733
  - Draximage model LS–1
  - Implant Sciences model 3500
  - IBt model 1251L
  - **IsoAid model IAI-125A**
  - Mentor model SL–125/SH–125

  - SourceTech Medical model STM1251
- Pd–103
  - Best Medical model 2335

The I–125 IsoAid model IAI-125A has been listed in boldface because it the model of seed primarily used for eye plaque brachytherapy at OHSU. OHSU uses I–125 for low–dose rate brachytherapy, but using Pd–103 is a future alternative is under consideration.

2.2. Description of the consensus data

The purpose of the consensus data is to provide consistent dosimetric calculations across the field. By standardizing dose calculation methods the field will be able to offer comparable quality of care with low–energy brachytherapy seeds. Adaption of consensus data will also allow research groups to compare their results to the literature without having to make several correction factors for the use of different data sets between studies.

The tables (Tables 2.1–2.4) in this section can be found in the TG–43U1S1. As IsoAid model IAI–125A seeds are primarily used for eye plaque brachytherapy at OHSU the data for that model is reported below. Data for additional seed models can be found in TG–43U1S1.

As per TG–43U1S1: "Interpolated data are **boldface**, extrapolated data are underlined, and *italicized* data are obtained from candidate datasets."[9]

Table 2.1: TG–43U1S1 Table I. NIST standard WAFAC calibration dates for air–kerma strength, and dose rate constant values.

Manufacturer	source type	Date used by NIST and ADCLs for calibration	${}_{CON}\Lambda$ $[cGy^{-1} * h^{-1} * U^{-1}]$
IsoAid IAI–125A	^{125}I	April 15, 2001	0.981

Table 2.2: TG–43U1S1 Table II. AAPM Consenus L, $g_L(r)$, and $g_P(r)$ values

	Line source approximation
L (mm)	3.0
r (cm)	IsoAid advantage IAI–125A
0.10	*1.040*
0.15	***1.053***
0.25	**1.066**
0.50	1.080
0.75	***1.035***
1.00	1.000
1.50	0.902
2.00	0.800
3.00	0.611
4.00	0.468
5.00	0.368
6.00	0.294
7.00	0.227
8.00	0.165
9.00	0.141
10.00	*0.090*
	Point source approximation
0.10	*0.686*
0.15	**0.833**
0.25	***0.967***
0.50	1.056
0.75	***1.029***
1.00	1.000
1.50	0.906
2.00	0.804
3.00	0.615
4.00	0.471
5.00	0.371
6.00	0.296
7.00	0.229
8.00	0.166
9.00	0.142
10.00	0.091
$\Phi_{an}(0.10)$	1.127
$\Phi_{an}(0.15)$	1.197
$\Phi_{an}(0.25)$	1.069
$\Phi_{an}(0.50)$	0.957
$\Phi_{an}(0.75)$	**0.962**

Table 2.3: TG–43U1S1 Table VII. F(r,θ) for IsoAid IAI–125A

	r [cm]					
Polar angle θ (degrees)	0.5	1	2	3	5	7
0	0.352	0.406	0.493	0.520	0.578	0.612
5	0.411	0.465	0.545	0.584	0.658	0.701
10	0.481	0.527	0.601	0.642	0.704	0.726
20	0.699	0.719	0.757	0.775	0.794	0.799
30	0.848	0.846	0.862	0.862	0.869	0.879
40	0.948	0.936	0.932	0.916	0.937	0.969
50	1.002	0.986	0.974	0.961	0.963	0.971
60	1.029	1.024	1.008	0.993	0.990	1.001
70	1.029	1.039	1.027	1.006	1.016	1.010
80	0.999	1.025	1.024	1.023	1.009	1.025
90	1.000	1.000	1.000	1.000	1.000	1.000
$\Phi_{an}(r)$	0.957	0.968	0.964	0.955	0.959	0.955

Table 2.4: TG–43U1S1 Table XI. Transverse plan dose rates as a function of distance

r [cm]	IsoAid Advantage IAI–125A
0.10	7.59E+1
0.15	4.35E+1
0.25	1.62E+1
0.50	3.97E+0
0.75	1.73E+0
1.0	9.50 E-1
1.5	**3.81E-1**
2.0	1.90E-1
3.0	6.40E-2
4.0	**2.77E-2**
5.0	1.39E-2
6.0	**7.72E-3**
7.0	4.37E-3
8.0	2.43E-3
9.0	1.64E-3
10.0	8.49E-4

2.3. Recommendations based on Task Group–129

Published in 2012, Task Group–129 (TG–129) examines how dose calculation formalisms created for radioactive sources could be applied to eye plaque brachytherapy. In particular, TG–129 focuses only on I–125 and Pd–103 seeds, but mentions alternative treatment methods in the appendix.

TG–129 methods assume full scatter conditions in an infinite homogeneous water medium calculated with the formalism described in TG–43U1 (see Section 2.1.3.). Aside from TG–43U1 formalism additional studies were conducted with Monte Carlo (MC) simulations. The goal of TG–129 was to not address treatment outcomes or give recommendations on specific seeds types and dose rates, but to address the implications of heterogeneity effects on delivering dose to the prescription point.

The report determined that 85 Gy delivered to 5.0 mm in homogeneous water only delivered 75 Gy and 69 Gy to the same point with I–125 and Pd–103 seeds, respectively, when accounting for heterogeneity corrections. The heterogeneity corrections include the attenuation effects of the gold–alloy plaque and Silastic insert, air–tissue interface, heterogeneity of ocular tissues and due to the shape of the eye, and the true scattering conditions on the surrounding medium. Accounting for these heterogeneities changes the dose calculation by up to 10% and thus a further discussion is needed with the radiation oncologist before implementing these changes.

Several factors affect the radiation transport across the eye such as the radionuclide used (I–125 vs. Pd–103), the location of the plaque (anterior vs. posterior), and the prescription point (2 mm vs. 5 mm). In order to ensure that the doses to the prescription point were being calculated in similar ways across all clinics, TG–129 recommends that users adopt the line–source approximations from TG–43U1 in homogeneous water. In addition to using line–source approximations, TG–129 recommends abandoning the 1D formalism and fully adopting the 2D formalism.

The 100 Gy originally prescribed with I–125 was based on dose calculation formalism created prior to the implementation of TG–43. The implementation of TG–43 resulted in a revised prescription dose of 85 Gy.

A desire to understand the heterogeneities within the eye were the focus of future reports, especially in regards to the heterogeneities caused by the COMS plaque. Several models of plaques and manufacturers have emerged, but the models with the most data are the COMS plaques.

As there is currently not treatment planning system that takes into account heterogeneities and is also approved by the FDA, TG–129 recommends a dual approach to treatment planning. The dual approach involves using TG–43U1's 2D formalism to make

calculations in homogeneous water and also accounting for heterogeneities in a TPS not approved by the FDA. For heterogeneity corrections, Plaque Simulator uses a superposition of single source distributions alongside additional corrections that are semianalytical in nature.

OHSU corrects for plaque heterogeneities using Plaque Simulator and compares the results to a spreadsheet method that is based on TG–43 dose calculation formalism without corrections for heterogeneities.

TG–129 recommends abandoning the 1D formalism for calculating doses and use the 2D formalism from TG–43U1.

3. Imaging modalities used for brachytherapy treatment planning

The two types of modalities used for diagnosising and planning eye brachytherapy cases are fundus (see Section 3.1.) and ultrasound imaging (see Section 3.2.).

At OHSU the physicist is given a treatment directive from the radiation oncologist and information regarding the tumor extent and location from the ophthalmologist. As a part of the diagnosis and treatment planning process ultrasound (US) and fundus images are taken for the patient and added to their file. The physicist has access to these images and can utilize them to create a treatment plan that accurately reflects the location and extent of the tumor.

Given the power of these imaging modalities to create an effective treatment plan it is worthwhile to discuss how each type of image is taken and what can be gleaned from each image. Although computed tomography (CT) and magnetic resonance imaging (MRI) are not typically used to diagnose or treat ocular melanomas at OHSU a brief discussion of how CT may be implemented in the future for treatment planning eye plaque brachytherapy cases is listed in Section 3.3. A discussion on MRI is not given. Although MRI offers excellent soft tissue contrast it lacks sufficient accuracy to be used to model the eye size or anatomy.

3.1. Fundus imaging

Fundus photography utilizes a flash of light through a dilated pupil to image the posterior portion of the eye. Specifically, fundus imaging gives an excellent view of the retina, optic head, and macula. A tumor and other pathology can be easily visualized in a fundus image (see Figure 3.1.).[17]

Fundus images for the patient should be available in AXIS.

3.1.1. Reading a fundus image

In addition to visualizing the tumor, the fundus image provides the most powerful tool in localizing the tumor within the treatment planning system. The placement of the tumor and other pathologies in the eye can be thought of as being a clock with the fovea in the

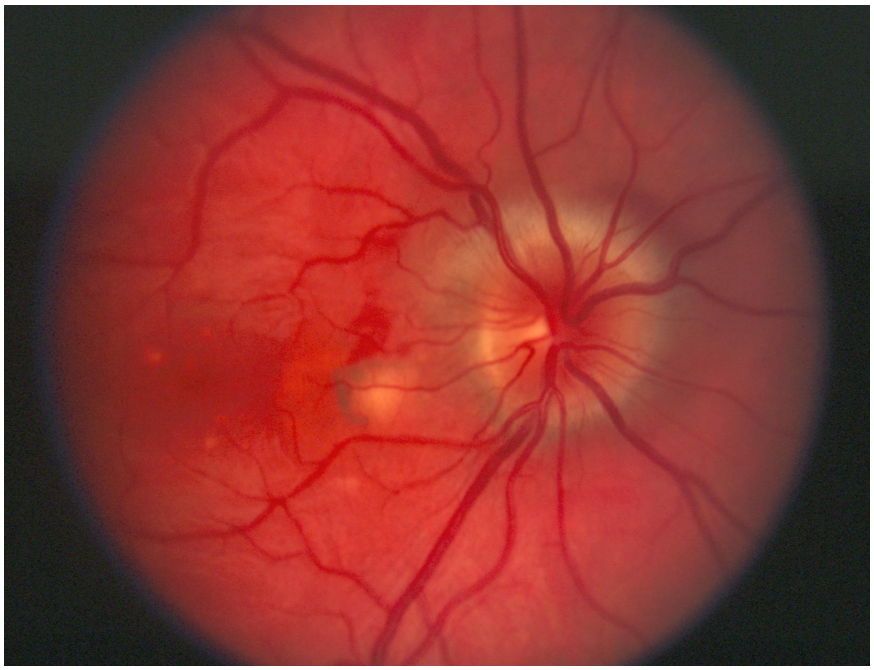

Figure 3.1: A fundus image prominently displaying the optic head. Image reprinted with permission from Medscape Drugs & Diseases (`http://emedicine.medscape.com/`), 2016, available at: `http://emedicine.medscape.com/article/1228681-overview`

center of the clock's face. Therefore, a pathology to due right of the fovea is said to be at the three o'clock position.

Plaque Simulator is able to model the tumor in the eye based off the fundus image if the distance between the optic head and fovea is given in the image. Calibrating the fundus image gives the physicist and intuitive and easy way to model the tumor location and should be utilized for future cases.

3.2. Ultrasound imaging

Ultrasound (US) is prominently used for diagnostic imaging due to its non-destructive, non-invasive, and relatively easy mode of operation. An advantage of US imaging is that it does not utilize ionizing radiation, removing the risk of secondary effects caused by ionizing radiation such as developing fatal cancer from the imaging process. For the treatment of ocular melanomas and other intraocular cancers ultrasound is utilized to localize the tumor and measure its dimensions.

US works by delivering a sound wave that propagates through the medium. Mechanical waves, such as sound and sonar signals, are a form of longitudinal compression waves that require a medium to travel through. The mechanical wave travels by creating alternating areas of compression and rareification called acoustic pressure. Acoustic pressure is measured in intensity, or power per unit area.

The mechanical wave originates from the probe of the US machine, called the transducer. The transducer creates a mechanical wave by applying an electrical voltage to piezoelectric crystals within the structure. The voltage causes the crystals to deform. The deformation of the crystals creates a mechanical wave. The mechanical wave has a frequency that is dependent on the size and shape of the piezocrystal, which higher frequency waves requiring thinner piezocrystal elements. Typically clinical ultrasound machines use frequencies of 2–15 MHZ.

At OHSU the ultrasonographers use transducers with frequencies of 10 MHz and 50 MHZ, respectively. The 10 MHz transducer creates waves that travel to the posterior portion of the eye and whose echoes travel back to the transducer to make a signal. The 50 MHz transducer is used to image tumors in the anterior portion of the eye. The larger frequencies of the 50 MHz means that the sound wave does not travel far before it is reflected back to the transducer. Although the 50 MHz waves do not travel as far as the 10 MHz waves, the 50 MHz waves are able to produce images with finer details.

The frequency of the ultrasound wave is constant as it travels throughout the body. As a wave hits a tissue interface there is a change in the wavelength, keeping the frequency of constant. The change in wavelength is because of the speed of sound is not uniform throughout the body. The speed of sound through various tissues is displayed in Table 3.1.

Table 3.1: The speed of sound through various tissues in the body

Material	Speed (m/sec)
Air	330
Soft tissue	1540
Fatty tissue	1450
Bone	4080

The relationship between frequency, the speed of sound, and wavelength is shown in Equation 3.1.

$$c\left[\frac{cm}{sec}\right] = \lambda\ [cm] * F\ [Hz] \tag{3.1}$$

The mechanical wave travels through the medium until it hits a tissue interface. An example of a tissue interface is between the tumor apex and intraocular fluid. Once a wave hits a tissue interface part of the wave reflected back to the transducer. The reflection of the wave reduces, or attenuates, the intensity of the original ultrasound beam.

The best image quality occurs at the focal zone of the ultrasound wave. The area between the transducer and the focal zone is called the near field or, more formally, the Fresnel zone. The Fresnel field is the region where the wavefronts gain the most coherence

with each other. Any area beyond the focal zone, distal to the transducer, is the far field. The far field is also called the Fraunhoffer zone. In the Fraunhoffer zone the ultrasound beam is diverging and the wavefront is losing coherence.

The resolution perpendicular to the ultrasound beam, or lateral resolution, is greatest at the focal zone. The ultrasound beam can be manipulated so that the focal zone is at the anatomy the physician is interested in imaging. In the case of ocular melanomas the focal zone is placed at the base or apex of the tumor.

The non-reflected part of the mechanical wave continues to propagate through the body, or is refracted. This refracted wave may be reflected back to the transducer when it reaches another tissue interface.

Once the mechanical wave returns to the transducer the mechanical energy deforms the piezocrystal. The deformation of the piezocrystal is recorded as a voltage.

This section describes the different modes of US imaging and how each mode is used to create an image. Section 3.2.2. focuses on the B–Mode of ultrasound and how basal and apex tumors dimensions are measured. In Section 3.2.3. there is a discussion on ultrasound biomicroscopy (UBM), which probes the anatomy with a higher frequency and gives finer anatomical information at shorter distances. UBM is predominantly used for imaging anterior tumors.

3.2.1. A–mode ultrasound

A–mode ultrasounds display echo strength over time and is ordered when an intraocular tumor is detected. A characteristic image of an A–mode ultrasound is shown in Figure 3.2.1.[18]

There are two types of A–mode US scans: biometric A–scans and standardized A–scans.

Biometric A–scans are used to obtain axial eye length measurements and have frequencies of 10–12 MHz.[2] This modality typically uses linear amplification to obtain an image.

Standardized A–scans detects and differentiates abnormal intraocular tissues. Using a lower frequency than biometric A–scans, standardized A–scans have a frequency of about 8 MHz and use an S–shaped amplification curve. This lower frequency allows the US waves to probe deeper tissues.

The echoes obtained from the US waves are normalized to the retinal echo. The retina is the most dense intraocular tissue and thus has the largest acoustic impedance. The greater the acoustic impedance the larger the echo that will be produced. Thus all other echoes and subsequent acoustic impedances are normalized to the retina.

Pathologies in the orbit will affect the presentations of A–mode scans. A–mode scans

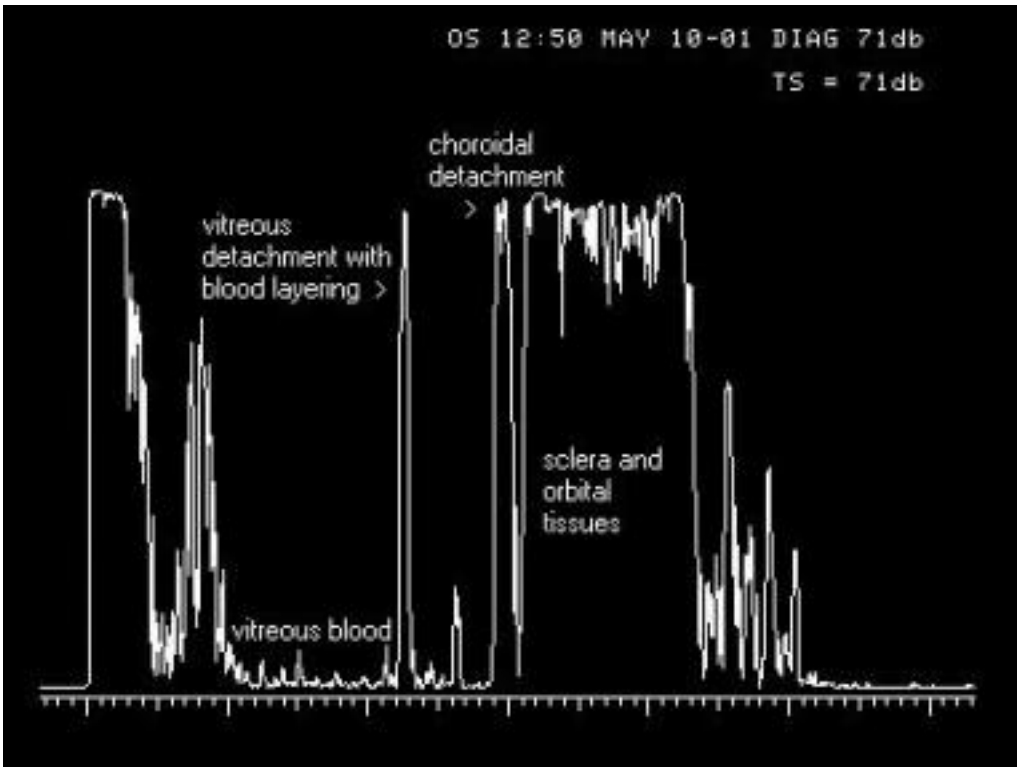

Figure 3.2: An example of an A–mode ultrasound image. Image reprinted with permission from Medscape Drugs & Diseases (`http://emedicine.medscape.com/`), 2016, available at: `http://emedicine.medscape.com/article/1228865-overview`.

can be used to measure the dimensions of a tumor or to diagnose macular degeneration. While A–mode scans are not used directly in the treatment planning process for eye plaque brachytherapy it is an important modality to diagnose and quantify several eye pathologies.

3.2.2. B–Mode ultrasound

Unlike A–mode US, which is inherently one–dimensional in nature, B–mode US is a two dimensional spatial representation of the orbit. This section deals primarily with standardized B–mode US, used to image the posterior portion of the orbit. The anterior portion of the orbit is imaged primarily with ultrasound biomicroscopy (UBM), which is dealt with in Section 3.2.3.

Standardized B–mode US use frequencies of around 10 MHz. The US shows the shape, location, and extent of intraocular tumors. An example of a B–mode US is shown in Figure 3.3.[18]

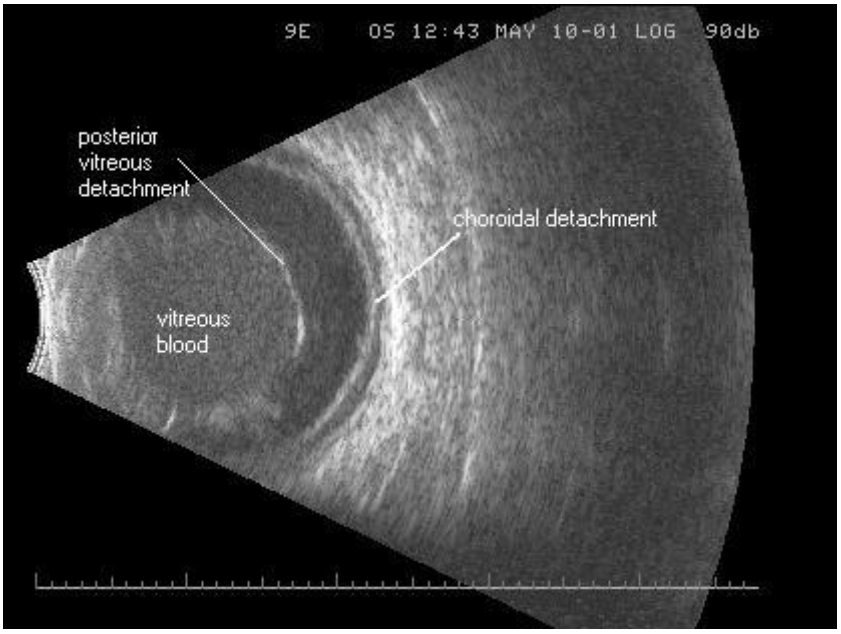

Figure 3.3: An example of an B–mode ultrasound image. Image reprinted with permission from Medscape Drugs & Diseases (`http://emedicine.medscape.com/`), 2016, available at: `http://emedicine.medscape.com/article/1228865-overview`.

The brighter a structure appears on the US the greater the structure's acoustic impedance; this is equivalent to having a high magnitude spike on an A–mode US. The acoustic impedances of the intraocular tumor will most likely be different than that of the retina and intraocular fluid, allowing the tumor to be imaged. If the tumor has a similar acoustic impedance to the retinal tissue then the displacement of the tumor apex from the retina can still be well–detected and visualized with B–mode US due to its irregular shape.

B–mode scans are obtained in two families of transducer probe orientations: axial scans and trans–scleral scans. Axial scans place the ultrasound probe directly on the cornea. Trans–scleral scans place the probe either perpendicular or parallel to the limbus, bypassing the cornea.

An example of an axial scan is shown in Figure 3.4.[18] Attenuation of mechanical waves through the lens results in poorer image quality than with trans–scleral scans. Trans–scleral scans are used most often to diagnose and quantify intraocular tumors due to their superior image quality and range of imaging potential.

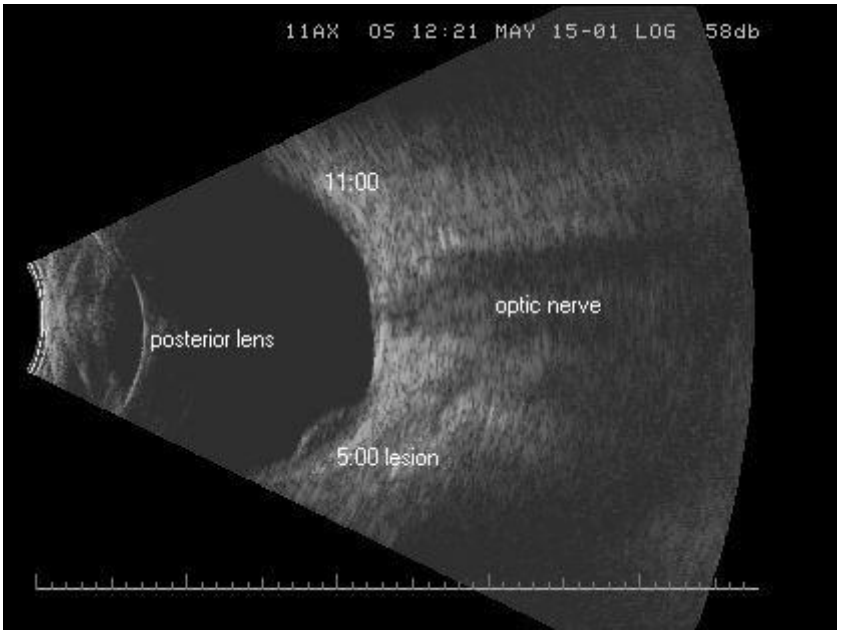

Figure 3.4: An example of an axial B–mode ultrasound image. Image reprinted with permission from Medscape Drugs & Diseases (`http://emedicine.medscape.com/`), 2016, available at: `http://emedicine.medscape.com/article/1228865-overview`.

Trans–scleral scans can be describes as either longitudinal or transverse scans.

The limbus is the part of the eye where color of the iris meets the white conjunctiva. The US probe contains a line that indicates the orientation of the beam. Longitudinal scans are created when the line on the US transducer is perpendicular to the tangent of the limbus. Only a single clock hour in the eye can be imaged with longitudinal scans.

The US probe for transverse scans occurs when the line on the US is parallel to the tangent of the limbus. Transverse scans detail the circumstantial extent of the intraocular tumor.

Reading B–mode ultrasounds

Similar to fundus images, ultrasounds are read by assuming a clock hour configuration with the face of the clock at the center of the fovea. US images will be labeled as "AX," "L," or "T" depending on whether or not the scan is axial, longitudinal, or transverse, respectively.

3.2.3. Ultrasound biomicroscopy (UBM)

Ultrasound biomicroscopy (UBM) is used to evaluate anterior structures with a 50 MHz probe. The mechanical waves produced by a 50 MHz probe only penetrate 5.0 mm and has a resolution of 37 μm.[2] Although the US waves are not able to penetrate as deeply as a standardized B–scan, the short wavelengths results in finer details of anterior structures.

Similar to standardized B–scans, UBM are able to image axial, longitudinal, and transverse scans.

Axial scans are imaged directly on the cornea, right over the pupil. Longitudinal scans are imaged with the probe perpendicular to the limbus and are the most common scan used for UBM. Transverse scans place the probe parallel to the limbus.

Reading a UBM image

Reading a UBM image is more intuitive than reading a B–mode US because the transducer is placed directly over the image of interest. Therefore an image taken at 3 o'clock means the transducer probe is placed at the 3 o'clock position of the eye and not the 9 o'clock position.

3.3. Computed Tomography (CT) imaging

Unlike fundus and US imaging, computed tomography (CT) imaging uses ionizing radiation. Ionizing radiation has the power to break chemical bonds and damage DNA. CT imaging is still considered a non–invasive form of imaging, but has greater risks than fundus and US imaging.

CT machines produce radiation through an x–ray tube, rotating the x–ray tube around and across the patient, creating a path like the rings of a slinky. The pieces are reconstructed with the rationale that the x–rays are attenuated differently though different materials.

Most diagnostic and planning CT images are taken at 100 or 120 kVp where there are both photoelectric and Compton interactions are present. The photoelectric effect occurs most often in high atomic number structures with low–energy photons. Compton interactions occur more readily with high electron density objects.

Diagnosing ocular melanomas with a CT machine is sub–optimal because most of the structures around and near the eye have a similar atomic numbers and electron densities. There is good contrast resolution between bone and normal tissue due to the difference in atomic number and electron density, but soft tissue contrast is relatively poor. Many of the cases of small to medium sized tumors can be easily imaged and diagnosed through

US and fundus imaging.

However, CT offers superior spatial position accuracy compared to fundus and US imaging in that the whole eye can be imaged all at once.

Plaque Simulator has the option to import CT images and calibrate the images. Calibrating the CT images can model the size of the eye. The size and eccentricity of the eye has some affect on the dose to the tumor and normal tissues and thus more accurate normal tissue measurements can be made by modeling the eye.

OHSU currently does not utilize CT images into its treatment planning process. There is a current move to using a calibrated fundus image to better position the tumor within the eye but not in modeling the eye size. An investigate should be launched to see if the eye dimensions can be discerned with an US probe. Meanwhile, it might be useful to utilize a former CT image of the eye if one is available. Unless the tumor is large enough that it significantly changes the shape of the eye older CT images can be useful since the eye does not grow significantly once it reaches its full size in puberty.

4. Creating a treatment plan in Plaque Simulator

The current method of planning eye plaque brachytherapy cases is through Plaque Simulator v5.9.3. Specifically, at OHSU there is a clinical computer that contains the software with this current version located within the physics resident's office.

Prior to planning a treatment for eye plaque brachytherapy the physicist will be given the following:

- A treatment directive from the radiation oncologist
- A medical note from the ophthalmic surgeon containing the tumor dimensions and plaque size
- An ultrasound image containing tumor dimension information
- A fundus image

All the information relating to the case should be available on the shared X:drive of the OHSU shared hospital drive.

Once the treatment planning system is opened the patient's name and medical record (MR) number are recorded in the treatment planning system. It is not required to enter the patient's gender or date of birth into the treatment planning system; this information will be available in other medical documents that accompany the treatment plan to the OR.

Indicate if the treatment site is the left or right eye. Verifying that the correct eye is being treated is an important part of the pre-surgical patient verification and a standard of care.

The eye plaque will always be a standard non–notched COMS plaque, unless stated otherwise by the ophthalmologist for posterior–based tumors. At OHSU a Silastic insert is loaded with seeds of a uniform seed distribution. In the event a notched plaque is used and the tumor is proximal to the optic then the seeds surrounding the optic disk may have a slightly higher activity to boost the radiation dose to the area.

COMS plaques are made out of a gold–alloy composition, trade name Modulay, which is composed of 77% gold, 14% silver, 8% copper, and 1% palladium by weight. The Silastic inserts that fit into the COMS plaque and hold the brachytherapy seeds are made out of 39.9% silicon, 28.9% oxygen, 24.9% carbon, 6.3% hydrogen, and 0.005% platinum by weight. The COMS plaque has a high atomic number ($Z_{gold} = 79$) relative to its

surroundings and thus experiences significant attenuation of photons through the photoelectric effect. The Silastic insert has a similar, but slightly larger, atomic number ($Z_{eff} \sim 11$) to water $Z_{eff} \sim 7.4$) and thus will also preferentially attenuate photons. Both the COMS plaque and Silastic insert cause significant heterogeneities that are not accounted for in simple homogeneous infinite water medium calculations. The heterogeneity effects are also made more severe by the low energy of the I–125 (average energy $\sim$ 28.5 keV) and Pd–103 (average energy $\sim$ 20.8 keV) brachytherapy seeds; with energies less than 30 keV the photoelectric effect is more prominent than Compton scatter in tissue.

The size of the COMS plaque size is determined by the ophthalmologist and is related to the basal dimensions of the tumor. COMS recommends selecting a plaque size that is 4 to 6 mm larger in diameter than the largest diameter of the tumor to give the tumor a 2 to 3 mm margin. However, the plaque size is ultimately at the discretion of the ophthalmologist who should explicitly specify the plaque size during the treatment planning process.

Notched COMS plaques have been created for posterior tumors proximal to the optic nerve. The notch allows the plaque to be placed around the optic nerve. Larger plaques are recommended for these cases; 2 to 6 mm larger in diameter than the non–notched plaques for a tumor of similar dimension but in a more anterior location. A plaque size should be selected that gives the tumor a 2 to 3 mm border around the tumor. Multiple seed strengths may be used to irradiate tumors proximal to the optic nerve near the notch of the plaque. Notched plaque sizes and using various seed strengths should be discussed with the ophthalmologist.

The original COMS study focused on plaques that ranged from 12 mm to 20 mm in 2 mm increments. However, COMS 10 mm and 22 mm plaques have been created. The number of radioactive seeds implanted in the COMS plaque depends on the size of the plaque with larger plaques accommodating more seeds than smaller plaques sizes. Seeds are arranged in polygon rings in order to deliver a symmetric dose as uniform as possible around the plaque location. The Silastic insert is designed to fit the surface of the eye. At OHSU the plaques are loaded with with IsoAid IAI–125U seeds.

IsoAid IAI–125U seeds have a 4.5 mm physical length made out of a titanium shell that is 0.05 mm thick. The shell's diameter is 0.8 mm thick. The active length, within the seed, is 3.00 mm with a 0.5 mm diameter. The active part of seed has a similar shape and geometry to the shell – a cylinder with a uniform distribution throughout the source. The source is made out of a silver halide, that is the radioactive I–125 is bonded with silver. The silver halide is a solid. In the event the seed becomes loose from the Silastic insert and breaks open only the broken pieces need to be collected without regard to

worrying about a powder.

The origin of the plaque–eye treatment coordinate system is the inner sclera of the eye. A prescription dose of 85 Gy is prescribed to the tumor apex plus a small margin for tumors whose radial length is less than 5 mm. However, treatment plans are simulated to a prescription dose of 86 Gy to ensure the tumor is adequately covered barring any uncertainty in implant and explant times. Tumors with radial lengths greater than 5 mm have the prescription point assigned at the tumor apex. A modified version COMS protocol for assigning the prescription point depth at OHSU is shown in Table 4.1.

Table 4.1: Current OHSU guidelines for determining prescription point depth depth based on tumor thickness since 2/11/2002

Tumor thickness	Prescription point depth
Less than 2.5 mm	3.0 mm inside sclera
2.5 to 2.9 mm	3.5 mm inside sclera
3.0 to 3.4 mm	4.0 mm inside sclera
3.5 to 3.9 mm	4.5 mm inside sclera
4.0 to 5.0 mm	5.0 mm inside sclera (same as COMS)
Greater than 5 mm	Actual apex of tumor (same as COMS)

Correction factors based on TG–43 formalism are listed below. Plaque Simulator simulates doses to the prescription point and normal tissues using a superposition of doses from all the seeds in the plaque. The dose contributions from individual seeds are based on TG–43U1 dose calculation formalism and consensus data. A full analysis of the dosimetric differences between Plaque Simulator and other treatment planning systems and methods are discussed in *Rivard et al. 2011.*[19]

4.1. Correction factors in Plaque Simulator

The correction differences between v5.3.9 and v6.3.1 at OHSU are listed below. Prior to accepting v6.3.1 the differences between these factors must be examined closely. If there were differences in values between the two versions then the differences were quantified and noted.

These factors can be turned on and off in the Prescription window of Plaque Simulator. Data sets for each version can be accessed in the Physics window.

4.1.1. Anisotropy

Anisotropy measures how much the dose rate changes as a function of distance and angle about the radioactive portion of the source. The default data set for v6.3.1 of Plaque

Simulator comes from *Solberg et al. 2002*[20] which is consensus data with a 91 element look up table. A copy of the consensus data can be found in TG–43U1S1 Table VII.[9]

Within this parameter are corrections for self–filtration, oblique filtration of primary photons through the encapsulating material, and scattering of photons in the medium.[7] The self–filtration of radiation causes the uneven dose distribution across the transverse axis of the seed. This parameter assumes that corrections from the geometry factor have been removed from this term.

4.1.2. Radial dose

Radial dose takes into account the fall off along the transverse axis due to absorption and scattering in the medium.[7] Plaque Simulator uses a line source approximation and uses the consensus data that is a combination of data from *Solberg et al. 2002*[20] and *Meigooni et al. 2002.*[21] A copy of the consensus data is found in Table II of TG–43U1S1.[9]

4.1.3. Scatter & Fluorescence

Corrections for scatter and fluorescence are not used for standard COMS plaques with a Silastic insert. This correction factor needs to be used if a gold insert is used instead of the Silastic insert and if something other than a COMS plaque is used.

The scatter and fluorescence correction is not turned on because it is assumed that these photons are absorbed by the Silastic insert before reaching the sclera. At OHSU only standard COMS plaques with Silastic inserts are used and this correction is not turned on.

4.1.4. Carrier factor

The carrier function takes into account the attenuation in the source carrier and is turned on for COMS plaques with Silastic inserts. In the case of the Silastic insert the effective atomic number ($Z_{eff} \sim 11$) is larger than that of water ($Z_{eff} \sim 7.4$). These atomic number differences cause heterogeneties that need to be corrected for dosimetric calculations.

The original correction factor, $T(r)$ was a constant of 0.9 for the central axis distances at 1 cm. *Chiu Tsao et al. 1993*[10] calculated $T(r)$ as a function of radial distance and linear attenuation coefficient.

However, when examining the carrier factor for v5.3.9 it became apparent the *Chiu Tsao et al. 1993* data set was not being used for this parameter. The differences between the data set for the carrier function is listed in Table 4.2 with r being the distance from the radioactive source in millimeters.

Table 4.2: The percent difference between v5.3.9 and v6.3.1 in the carrier factor

r(mm)	T(r) of v5.3.9	T(r) of v6.3.1	% difference
0	1.0000	0.9220	-7.80
1	0.9710	0.9210	-5.15
2	0.9510	0.9190	-3.36
3	0.9320	0.9150	-1.82
4	0.9140	0.9100	-0.44
5	0.8980	0.9050	0.78
6	0.8840	0.8990	1.70
7	0.8710	0.8920	2.41
8	0.8590	0.8860	3.14
9	0.8480	0.8800	3.77
10	0.8390	0.8740	4.17
11	0.8310	0.8680	4.45
12	0.8240	0.8630	4.73
14	0.8130	0.8530	4.92
16	0.8050	0.8450	4.97
18	0.8010	0.8380	4.62
20	0.8000	0.8330	4.12
25	0.8000	0.8220	2.75
30	0.8000	0.8160	2.00
40	0.8000	0.8080	1.00

The most notable difference is at $r = 0$ mm which has a percent difference of –7.80%. This large percent difference will affect the differences in dose calculations between v5.3.9 and v6.3.1 for small distances, especially the scleral doses.

Dosimetry at small distances near radioactive sources is extraordinarily tricky due to the steep dose gradient and the close proximity of the treatment volume to critical eye structures. Although the *Chiu Tsao et al. 1993* data set may not be perfect, it will allow OHSU to calculate small doses in a way that is consistent to other clinics that also implement the same data set. Therefore the *Chiu Tsao et al. 1993* data set shown in v6.3.1 should be adopted. The adoption of the *Chiu Tsao et al. 1993* data set may result in sclera doses percent differences larger than 5% between v5.3.9 and v6.3.1.

4.1.5. Air scatter

The air scatter term takes into account the reduced scatter near air interfaces and is negligible at distances beyond 1.5 cm (15 mm) from the air interface. This correction factor is turned on for some anterior tumors, but is turned off by default.

In v5.3.9 the air scatter correction factor is calculated using Equation 4.1 originally

derived from *de la Zerda et al. 1996.*[22]

$$A(R) = a_1 + (a_2 * R) \tag{4.1}$$

- distance from air boundary, R
- $a_1 = 0.850$
- $a_2 = 0.100$

Equation 4.1 applies for distances less than 15 mm from the air interface.

In v6.3.1 the air scatter correction factor data set is from *Thomson et al. 2008.*[6] As with v5.3.9 and Equation 4.1 this correction factor becomes negligible at distances greater than 15 mm from the air interface.

The percent differences between v5.3.9 and v6.3.1 for the air correction factors is shown in Table 4.3.

Table 4.3: The percent difference between v5.3.9 and v6.3.1 in the air correction factor

R(mm)	A(r,d) for v5.3.9	A(r,d) for v6.3.1	% difference
0.0	0.8500	0.9200	8.24
0.5	0.8550	0.9400	9.94
1.0	0.8600	0.9680	12.56
2.0	0.8700	0.9900	13.79
3.0	0.8800	0.9950	13.07
4.0	0.8900	0.9980	12.13
5.0	0.9000	1.0000	11.11
6.0	0.9100	1.0000	9.89
7.0	0.9200	1.0000	8.70
8.0	0.9300	1.0000	7.53
9.0	0.9400	1.0000	6.38
10.0	0.9500	1.0000	5.26
11.0	0.9600	1.0000	4.17
12.0	0.9700	1.0000	3.09
13.0	0.9800	1.0000	2.04
14.0	0.9900	1.0000	1.01

This difference in data is shown in Figure 4.1, which is Figure 8 of *Thomson et al. 2008*[6]. Figure 4.1 also shows the trend line from Equation 4.1 that was originally listed in *de la Zerda et al. 1996.*[22]

In Figure 4.1 the upper graph (a) measures the air correction factor at the posterior pole. The y parameter within graph (a) measures the air correction factor as affected by the off–axis factor. The lower graph (b) has the plaque placed at the equator with the z parameter measuring air correction factor with the distance from the plaque. As underlined in both of these graphs (Figure 4.1) the air correction factor depends on the

location of the plaque and distance from the air interface.

As is the case with the carrier factor in Section 4.1.4. it is important to note that these large percent differences are due to use of different data sets. It is recommended that the data from *Thomson et al. 2008* be implemented for clinical use despite its large percent differences from the data found in *de la Zerda et al. 1996* as *Thomson et al. 2008* uses data from Monte Carlo simulations.

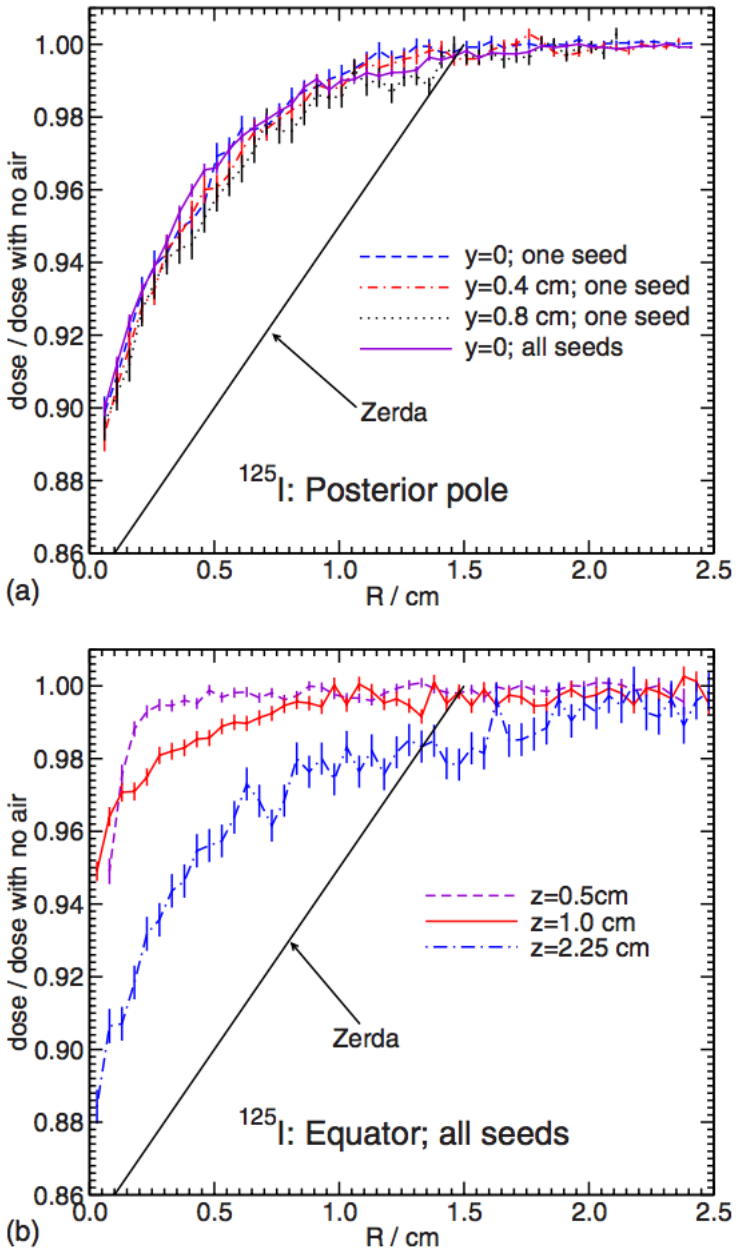

Figure 4.1: Figure 8 from Thomson et. al 2008 that shows the differences between Monte Carlo and previous data from de la Zerda et al. 1996.

5. Methods

The rationale and methods used for this thesis are described in the sections below. The methods used to compare the dosimetric difference between Plaque Simulator versions 5.3.9 and 6.3.1 is described in Section 5.1. The methods used to compare one–dimensional (1D) to three–dimensions (3D) planning in Plaque Simulator v6.3.1 are listed in Section 5.2.

5.1. Comparison between Plaque Simulator v5.3.9 and v6.3.1

The main task in accepting and commissioning a new treatment planning system is to understand how the new system deviates from the old system. A challenging aspect of brachytherapy dosimetry is its steep dose gradients and the close proximity (∼1 mm) of critical structures to each other and the source. Therefore a large task in accepting and commissioning v6.3.1 of Plaque Simulator is to test how it calculates doses to the prescription point, sclera, and tumor apex compared to v5.3.9.

The method for testing the dosimetric differences between v5.3.9 and v6.3.1 was to recreate patient plans originally made in v5.3.9 with v6.3.1. Patients treated in 2015 and 2016 were selected to be replanned with the new treatment planning system. Five patients (n=5) were selected for each non–notched COMS plaques 14, 16, 18, 20, and 22. Only three patients (n=3) were selected for a notched COMS 20n study because there were only three patients treated with notched plaques in 2015 and 2016. There were no patients treated with COMS 10 or 12 non–notched plaques in 2015 and 2016 at OHSU. Overall twenty–eight (n=28) cases were selected for this study.

Plans were recreated v6.3.1 with the exact information used in v5.3.9 which includes tumor dimensions from ultrasound (US) images and the prescription point and dose prescribed by the radiation oncologist. The prescription point is specified to the tumor apex plus a small margin and follows the COMS protocol; tumors with radial diameters greater than 5 mm prescribe the prescription dose to the tumor apex. The tumors were centered on the equator at the 9 o'clock hour. Each case had the plaque centered directly over the base of the tumor with the tumor modeled as a standard shape.

The COMS plaque size is prescribed by the ophthalmologist. The number of seeds

used depends on the COMS plaque size and whether or not the plaque is notched. The plaque is loaded with a uniform distribution of seeds throughout the plaque. An implant time of 100 hours is prescribed with IsoAid IAI-125U seeds.

Special attention was paid to the calculation parameters used to create the plan. Some anterior–based tumors required air corrections. The new (v6.3.1) plans were double checked and carefully compared to the old (v5.3.9) plans to make sure that the same dosimetric parameters are used between treatment plans.

Additional double checks between plans include confirming the tumor dimensions and that the correct eye was modeled. Copies of the old and new treatment plan reports are available in OHSU's X:drive folder.

Once the new (v6.3.1) treatment plans were created the seed strengths, doses to different distances within the eye, and normal tissue doses were recorded. Prior to recreating the treatment plans, the same parameters from v5.3.9 were recorded. The percent difference between v5.3.9 and v6.3.1 was calculated using Equation 5.1.

$$\text{percent difference} = \left(\frac{\text{new dose} - \text{old dose}}{\text{old dose}}\right) * 100\% \tag{5.1}$$

The percent difference to doses to the prescription point, sclera, and tumor apex were recorded and examined.

The prescription point is determined by the tumor apex. If the tumor apex is less than 5 mm then the prescription point is to the tumor apex plus a small margin. If a tumor is greater than 5 mm in radial length then the prescription point is to the apex of the tumor.

The COMS protocol recommends a prescription dose of 85 Gy over 3–7 days. At OHSU the implant time is roughly 100 hours. In order to better reach the prescription dose of 85 Gy, physicists at OHSU create treatment plans at a prescription dose of 86 Gy. This discrepancy in time takes into account wiggle room between proposed implant times (based on surgical start times) versus actual implant times.

Some of the cases in the study had implants that were not 100 hours or had prescription doses that were not 86 Gy. This may be due to the only plans that were available for a patient were postplans that reflected the actual amount of time the plaque was implanted in the patient and not the preplan. Some plans also had a preplan implant time of 101 hours as the previous explant time was 2:00 p.m. (as opposed to the current 1:00 p.m.) on a Friday.

The sclera is the a part of the outermost layer of the eye and does not include the optic nerve or the cornea. Dose to the sclera is unavoidable as gamma–rays must transverse the sclera to reach the tumor. Plaque Simulator models the sclera to have a thickness of

1 mm.

The tumor apex is the most distal radial distance of the tumor from the sclera. Sometimes the prescription point is at the tumor apex if the radial distance is greater than 5 mm. However, tumors with a radial distance less than 5 mm will have a small margin between the tumor apex and prescription point.

A shortcoming to this study is that the effect of the distance of the tumor apex and prescription on the percent difference between v5.3.9 and v6.3.1 was not examined. An investigation should be launched that selects patients from OHSU that have different tumor apex heights within the same COMS plaque size and style.

The range of tumor apex heights is listed in Table 5.1.

Table 5.1: The COMS plaque size and style and range of tumor apex heights from a study of n=28 patients comparing the percent difference in dose

COMS plaque size	Range of tumor apices in group (mm)
14	2.00–3.50
16	1.60–2.90
18	1.00–4.20
20	1.90–7.60
20n	1.10–3.50
22	3.40–6.70

Patients were selected for this study based solely on their COMS size and style without regard to the height of their tumors. A future study will take into tumor height to see if there is a relationship between the percent difference between v5.3.9 and v6.3.1 in regards to the prescription point, sclera, and tumor apex.

Ideally the percent difference between these parameters should be less than 5% in order to successfully accept and commission v6.3.1 into clinical use.

5.2. Comparison between 1D and 3D planning in v.6.3.1

A goal of the clinical medical physicist is to understand the radiation delivered to both the tumor and normal tissue. However, the current method of treatment planning at OHSU involves one–dimensional (1D) planning, where a treatment plan focuses only on irradiating the tumor without concern to the normal tissues. For 1D planning the tumor is placed at the 9 o'clock hour, centering the equator, and not at its true clock hour or latitudinal position.

Patients are informed that they may experience vision loss or deterioration, especially for tumors proximal to the macula and optic nerve.

Understanding the types of doses that normal tissues receive in the course of eye plaque brachytherapy, in addition to providing better informed consent to the patient, can also help OHSU understand the correlation between doses and normal tissue toxicity. Radiation biology is a continually growing field with no absolute clinical answers regarding how a patient will react to radiation. Therefore, in order for OHSU to successfully and accurately contribute to the knowledge on how radiation affects normal tissues in the eye, accurate measurements of radiation to the eye need to be recorded. Three–dimensional (3D) planning will help OHSU achieve this goal by placing both the tumor and plaque in a location more proximal to where the tumor is located in the patient.

In order to understand how positioning with 3D planning methods the tumor will affect normal tissue doses the v6.3.1 Plaque Simulator 1D plans created for the comparison between v5.3.9 and v6.3.1 were copied. Creating a copy of the original v6.3.1 1D plan ensures that the 3D plan was exactly the same as the 1D plan, minus the position of the tumor and the position of the COMS plaque. This method minimizes the impact of human error and saves time as the 3D plan does not have to be created by scratch. Duplicating the 1D plan will save time in the future and will allow the physicist and physician to compare the two plans to each other if more stringent normal tissue estimates need to be made.

To reflect the treatment planning was focused on 3D planning the patient name was changed from "LASTNAME, FIRSTNAME 1D" to "LASTNAME, FIRSTNAME 3D." A new seed inventory was also created to reflect this change. As the seed strength may change with the move from 1D to 3D planning it is recommended that the physicist delete the seed inventory that is not used as to more accurately reflect the true seed inventory of the facility once a treatment plan is selected.

Once the 3D treatment plan was created, with the patient name and seed inventory changed, the physicist will examine the patient images and physician notes to determine the position of the tumor.

Ocular imaging is best thought of as a giant clock with the fovea being in the center of the clock face. Tumors that are directly superior to the fovea, regardless of whether the tumor is located in the left or right eye, is always said to be at the 12 o'clock position. Likewise, tumors located to the right (viewer's right, patient's left) of the fovea are read as in the 3 o'clock position.

Physician notes may include either clock hours or anatomical locations, such as inferonasal or superotemporal. The anatomical references have a corresponding general clock hours and thus a clock hour may be estimated if relative anatomical references are given. Fundus images are the most intuitive for understanding the relative clock hour and location, but ultrasound (US) images may explicitly label the tumor's clock hour.

US images should be labeled with the clock hour and orientation of the ultrasound probe. The US images are used primarily to understand the shape and dimensions of the tumor.

For the 3D study two US images and one fundus image were added to Plaque Simulator. To easily upload the patient images, label the US images "US" and "US2," respectively, and the fundus image "fund" and save these all images in the same folder as the treatment plan. Plaque Simulator gives an "Upload All" option when the US icon image is right clicked in the Retina window.

Once all the images were uploaded the fundus image could be calibrated to the treatment planning system. If the physician labels the distance between the macula and optic head, the physicist can make a note of the distance in the treatment planning system. Once the fundus image is calibrated the fundus image will be superimposed on the retina window.

Plaque Simulator gives the option to drag the tumor to the proper location in the retina window. The tumor dimensions, which were obtained from the US images, are unchanged from the 1D plan. The tumor was dragged to match its apparent location in the fundus image. Once the tumor was placed in its approximate location then the tumor can be centered by the clock hour within the retinal window.

If the fundus image was not calibrated then it is not possible to superimpose the image onto the retinal window. Therefore a best guess was made as to where the tumor was located based on the fundus image. The clock hour location is easy to discern from the fundus image and physician notes, but the real challenge in 3D planning is understanding the anterior/posterior location. Calibrated fundus images will make the treatment planning process simple as it helps the physician locate both the clock hour and latitude.

Once the tumor is placed the plaque is repositioned to be centered directly on the tumor. The same prescription dose is prescribed to the same point with Plaque Simulator recalculating seed strengths. The treatment plan is saved and the doses to the normal tissues are recorded.

The 1D and 3D treatment plans are compared to each other and examined for how much they deviate in doses to the tumor and normal tissues The percent difference between the two plans is the same equation used to examine the difference between v5.3.9 and v6.3.1 and is listed in Equation 5.1.

It is important to note that this study is establishing proof of concept. The tumor positions are "best guesses" based on the physician notes and fundus images. The tumor positions should be taken with a grain of salt and were not placed based on calibrated fundus images. Ideally calibrated fundus images would have been used to place the tumor

in the correction position. Fundus images with the distance between the macula and optic head were not labeled for most of the patients.

However, the distribution of tumor locations and placements based on the uncalibrated fundus images allowed a diversity of tumor locations. This diversity of tumor locations included both anterior and posterior tumors across each of the clockhours. From a theoretical standpoint the "best guess" tumor locations will still demonstrate proof of concept for 3D planning.

The percent different for the doses to the prescription point, sclera, and tumor apex were calculated and discussed in the following chapters. Given the corrections for heterogeneities remained constant the percent differences were minuscule for the parameters examined below. The standard for acceptable percent differences in modern medical physics is less than 2% for calculation with similar methods.

6. Results

The results for the study examining the differences between Plaque Simulator v5.3.9 and v6.3.1 are listed in Section 6.1. Likewise, the results of the study comparing 1D to 3D planning are listed in Section 6.2.

6.1. Comparison between Plaque Simulator v.5.3.9 and v.6.3.1

The results of the study comparing the doses to the prescription point, sclera, and tumor apex are shown in the following pages. The x-axis indicates the size and style of plaque.

The y-axis represents the percent difference between versions 5.3.9 and 6.3.1. A positive percent difference indicates that v6.3.1 calculates a higher dose than v5.3.9. A negative percent difference indicates that v6.3.1 calculates a lower dose than 5.3.9.

6.1.1. Prescription point

The results of the percent difference of doses to the prescription point are shown in Figure 6.1.1.

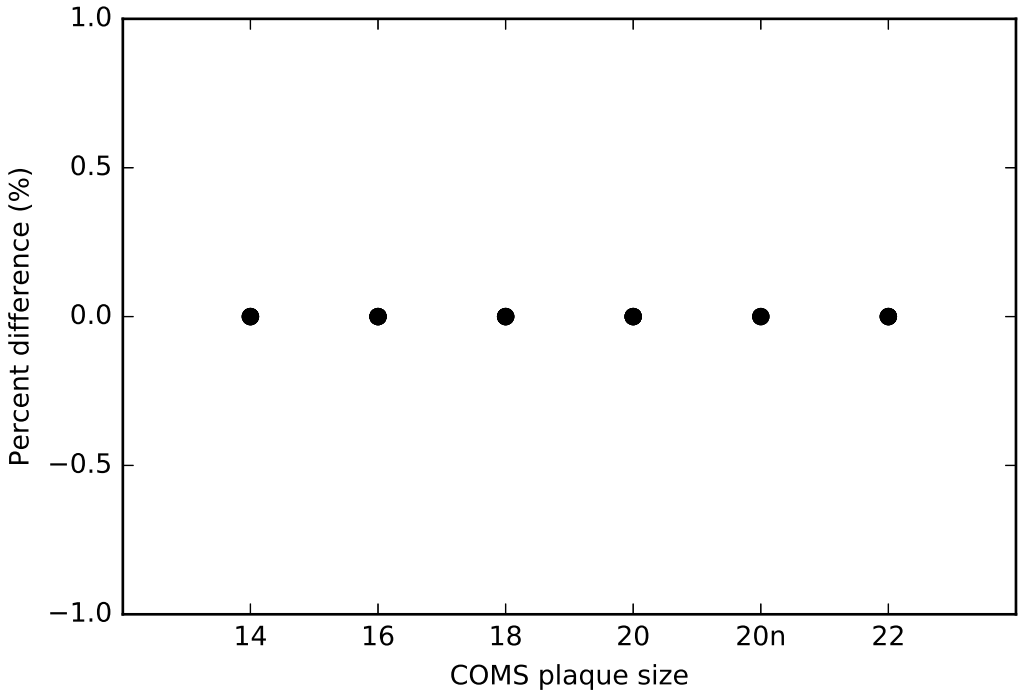

Figure 6.1: A comparison of the percent difference between the dose to the prescription point between Plaque Simulator versions 5.3.9 and 6.3.1.

6.1.2. Sclera

The percent difference in doses to the sclera are shown in Figure 6.1.2.

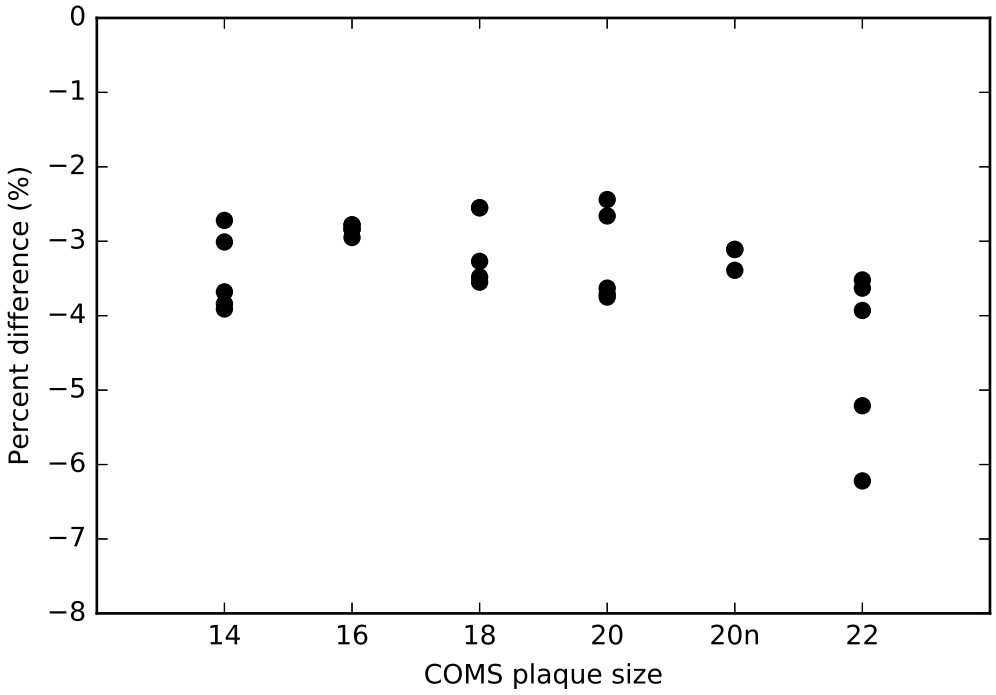

Figure 6.2: A comparison of the percent difference between the dose to the sclera between Plaque Simulator versions 5.3.9 and 6.3.1.

6.1.3. Tumor apex

The results of the percent difference in doses to the tumor apex between v5.3.9 and v6.3.1 are shown in Figure 6.1.3.

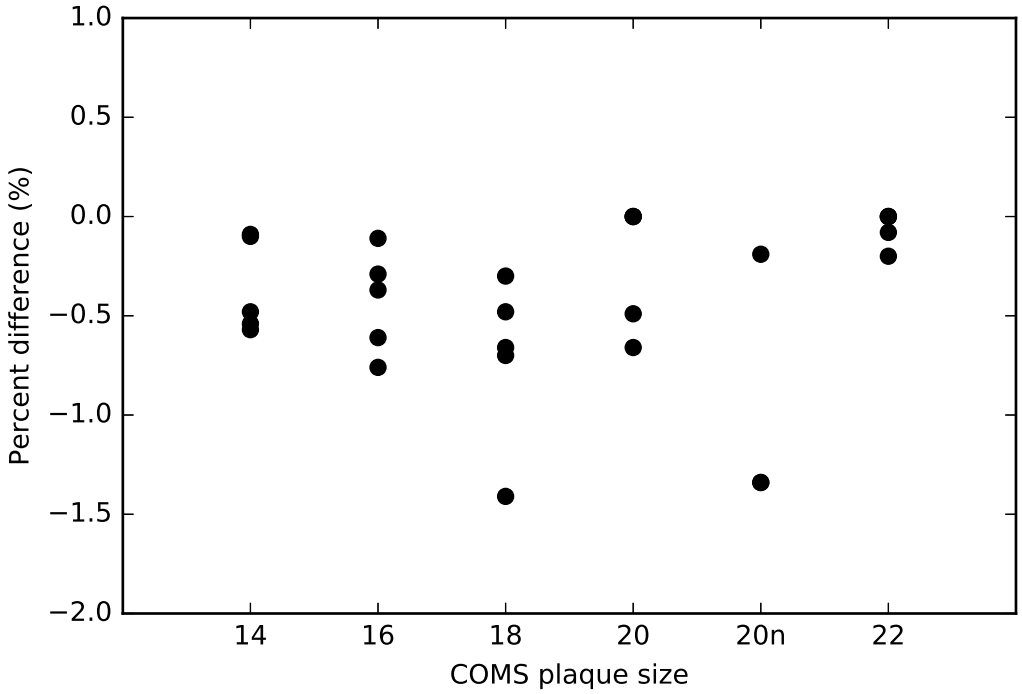

Figure 6.3: A comparison of the percent difference between the dose to the tumor apex between Plaque Simulator versions 5.3.9 and 6.3.1.

6.2. Comparison between 1D and 3D planning in v.6.3.1

The results of the study comparing the doses to the prescription point, sclera, and tumor apex are shown in the following pages. The x-axis indicates the size and style of plaque.

The y-axis represents the percent difference between versions 5.3.9 and 6.3.1. A positive percent difference indicates that v6.3.1 calculates a higher dose than v5.3.9. A negative percent difference indicates that v6.3.1 calculates a lower dose than 5.3.9.

6.2.1. Prescription point

The percent difference between 1D and 3D planning to the prescription point is shown in Figure 6.2.1.

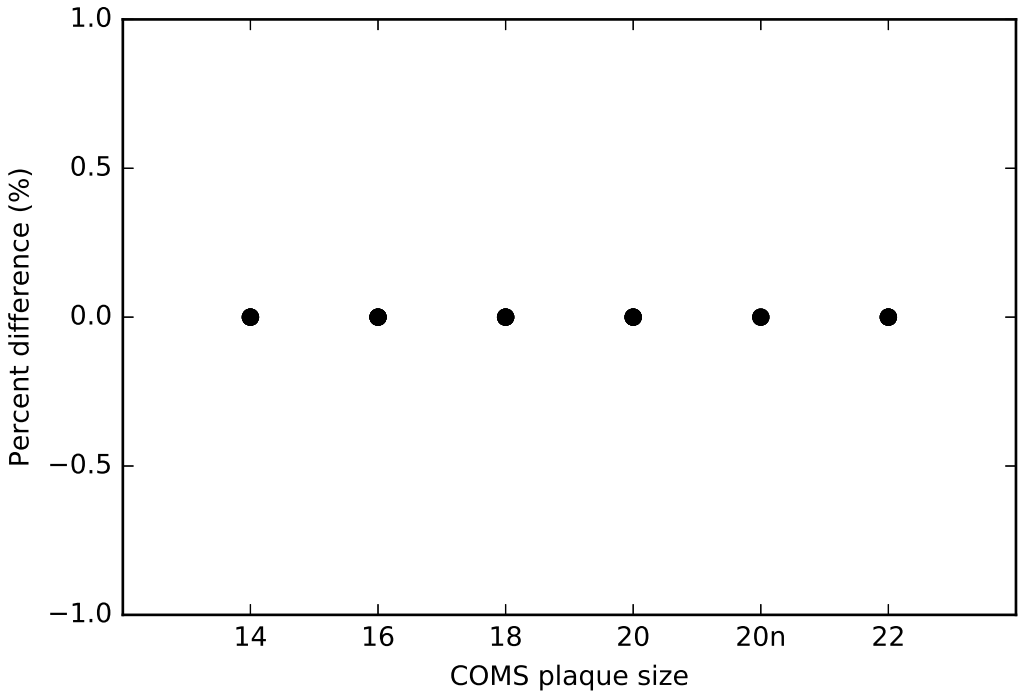

Figure 6.4: A comparison of the percent difference between the dose to the prescription point between 1D and 3D treatment planning methods.

6.2.2. Sclera

The results of the percent difference to the sclera due to the use of 3D planning versus 1D planning is shown in Figure 6.2.2.

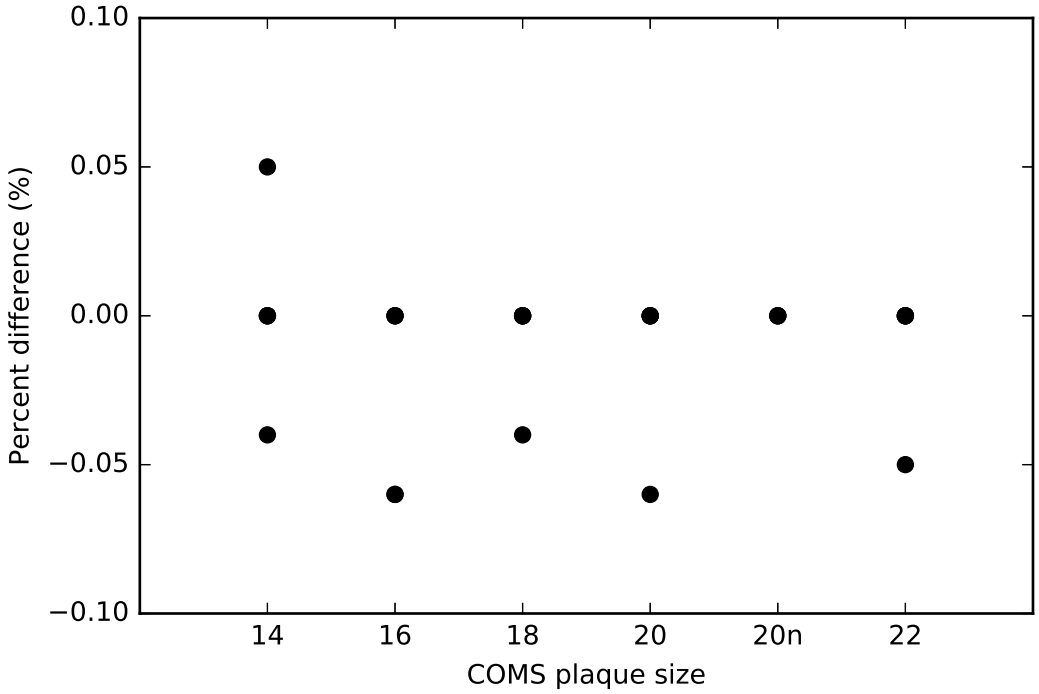

Figure 6.5: A comparison of the percent difference between the dose to the sclera between 1D and 3D treatment planning methods.

6.2.3. Tumor apex

The results of the study examining the percent difference in the tumor apex between 1D and 3D planning are shown in Figure 6.2.3.

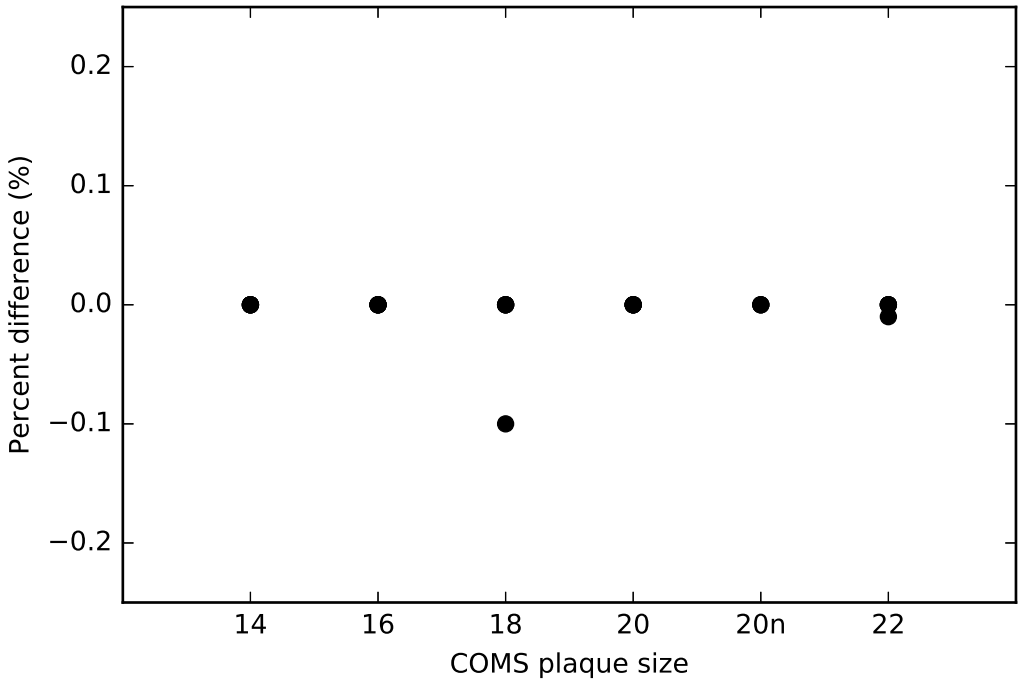

Figure 6.6: A comparison of the percent difference between the dose to the tumor apex between 1D and 3D treatment planning methods.

7. Discussion

A discussion of the dosimetric and technical differences between v5.3.9 and v6.3.1 are listed in Section 7.1. The dosimetric differences between the one–dimensional (1D) and three–dimensional (3D) planning methods in Plaque Simulator v6.3.1 are described in Section 7.2.

7.1. Comparison between Plaque Simulator v5.3.9 and v6.3.1

Aside from two COMS 22 non–notched cases, the prescription point, sclera, and tumor apex percent differences were less than 5% for 93% (26 out of 28) of cases. Each parameter is further investigated below. Section 7.1.1. discusses percent differences to the prescription point, Section 7.1.2. to the sclera, and Section 7.1.3. to the tumor apex.

7.1.1. Prescription point

As seen in Figure 6.1.1. there was a 0% difference between v5.3.9 and v6.3.1 for all cases (28 out of 28). Plaque Simulator creates its treatment plans based on the doses to the prescription point, which means these results are trivial and are expected to remain the same from v5.3.9. As trivial as these results are they are important for establishing a control for the rest of the study.

If there was a difference in the dose to the prescribed point then it is most likely a human error that needs to fixed. Ideally the dose to the prescription point should not change from patient to patient if the treatment protocol is being followed consistently.

7.1.2. Sclera

There are two trends of note: v6.3.1 consistently calculates a lower dose to the sclera than v5.3.9 and most of the percent difference appears to be within 2–4% between v5.3.9 and v6.3.1.

Most of the cases (26 out of 28; 93%) calculated values within 5% between v5.3.9 and v6.3.1. The two cases that exceed a 5% percent difference have values of –5.21% and –6.22%, respectively.

These large percent differences are due to the change in data for carrier factor correction between v5.3.9 and v6.3.1. In v5.3.9 data is taken from an unknown data source and v6.3.1 uses a data set listed in TG–129[1] from *Chiu Tsao et al. 1993*.

The carrier factor correction at the radioactive seed ($T(r)$ at $r = 0$ mm) for v5.3.9 was 1.000, which is a –7.8% difference from 0.9220 for v6.3.1. At $r = 1$ mm the $T(r)$ factors are 0.9710 and 0.9210 for v5.3.9 and v6.3.1, respectively, a –5.15% difference. Given the large difference between these two data sets at 0 mm and 1 mm it is reasonable and apparent that the doses to the sclera will be significantly affected.

Regardless of the large percent dose differences between the two carrier correction data sets v6.3.1 should be accepted.

7.1.3. Tumor apex

Similar to the sclera percent differences, v6.3.1 appears to predict smaller doses than v5.3.9. All of the cases either predict no percent difference between v5.3.9 and v6.3.1 (6 out of 28; 21%) or a decrease in dose.

Of the cases that predict a decrease in dose to the tumor apex, 68% (19 out of 28) of cases show a percent difference of less than 1%. The remaining three cases have a percent difference less than 1.5%. The percent difference for tumor apex between v5.3.9 and v6.3.1 are all below 1.5%, much lower than the standard of 5% used in medical physics.

The percent difference in the carrier factor correct data set is less dramatic farther away from the sclera, meaning the tumor apex doses will be less dramatically affected by the dissonances in v6.3.1's data from v5.3.9. Given the small percent difference the change in doses to the tumor apex this data should not be a concern in implementing v6.3.1 into clinical use.

7.2. Comparison between 1D and 3D planning in v.6.3.1

Section 7.2.1. discusses how the dose to the prescription point changes, Section 7.2.2. discusses doses to the sclera, and Section 7.2.3. talks about how doses to the tumor apex are affected by 1D vs 3D planning.

7.2.1. Prescription point

As shown in Figure 6.2.1., the dose to the prescription point is not affected by repositioning the tumor. The relative percent difference shows if the doses are increasing or decreasing between v5.3.9 and v6.3.1.

This is an expected result as the treatment plan is created based on a prescribed dose to the tumor apex plus a small margin. Any deviation from this result is on behalf of human error and not the treatment planning system. If a spreadsheet is created that compares the percent different between treatment plans then it is recommended that the prescription point percent difference is included as a safety check that the same dose is being delivered.

7.2.2. Sclera

Twenty-one out of 28 cases (75%) had unchanged doses to the sclera. However, the cases that did have a change to the sclera usually had a decrease in estimated dose. The largest percent difference was no greater than 0.06%.

The change in the dose to the sclera may be related to the position of the tumor.

Some anterior tumors may present as a pigmented fragment within the iris. In these cases the plaque would cover part of the cornea and limbus and less of the sclera. Five out of seven cases with non-zero percent differences are anterior tumors have an increased dose to the lens. The 3D planning method estimates an 68.79%–433.85% increase in dose to the lens for these cases.

The remaining two cases showed a non–zero and decrease in lens dose, but an increase of dose to the macula of 5.03% and 274.17%, respectively. Some tumors may be so posterior that the plaque covers parts of the optic disc and macula. These tumors will often require a notched plaque that is conformal to the optic nerve.

While it is important to understand why the sclera dose is affected by tumor position the percent difference between 1D and 3D planning negligible and should not be a concern to adapting 3D planning.

7.2.3. Tumor apex

Most cases (26 out of 28; 93%) had no change in the tumor apex between 1D and 3D planning processes. The two cases that showed deviation had percent differences of 0.1% and 0.01%, respectively.

There are several explanations for the change in tumor apex dose. One case is an anterior lesion and the other is a posterior lesion with both cases showing decreased doses to the sclera. The inhomogeneities of the anterior and posterior lesions of the eye may be affecting radiation transport to the prescription site. These inhomogeneities require sources of slightly different activities which means the radiation will not distribute itself exactly the same between the 1D and 3D cases.

The percent differences of less than 0.1% should not be a concern in implementing

3D planning systems into clinical practice.

8. Proposed future studies for eye plaque brachytherapy

Given medicine is a practice that is continually growing there are still ways to improve the treatment and quality assurance of eye plaque brachytherapy at OHSU. Listed below are a few areas to investigate in the future.

8.1. Repeat analysis between v5.3.9 and v6.3.1 with varied tumor thicknesses

The COMS plaque size and style is ultimately determined by the ophthalmologic surgeon. The COMS plaque size is determined by the largest basal diameter with COMS protocol recommending a margin of 2 mm between the edge of the COMS plaque and the tumor edge on either side. However, the ophthalmologic surgeon may choose a larger COMS plaque size in order to be comfortable with tumor coverage.

The seed strength is dependent on the axial length of the tumor; tumors with larger apices or farther prescriptions points require larger seed strengths. For this thesis the effect of the prescription distance on doses between v5.3.9 and v6.3.1 was not considered. However, a study should be conducted investigating how the doses between v5.3.9 and v6.3.1 change in respect to the prescription point distance for each COMS plaque size.

Medical records from patients who have undergone eye plaque brachytherapy should be examined with the COMS plaque size, tumor dimensions, and prescription point distance being recorded. Ideally, for each plaque size there should be patients selected whose tumor apex height corresponds to distances of 1.00 mm, 1.50 mm, 2.00 mm, etc. Cases originally planned in v5.3.9 should be replanned in v6.3.1 with doses to prescription point, sclera, and tumor apex being recorded. The percent difference between v5.3.9 and v6.3.1 should be recorded to see if there is a relationship the tumor apex distance and the percent difference.

The tumor dimensions for each of the cases (n=28) comparing v5.3.9 to v6.3.1 are recorded in the data set available on the X:drive.

8.2. Implementation of Palladium–103 seeds

There have been many studies investigating the relationship between radionuclide and normal tissue toxicities. Of particular interest, Pd–103 has been compared to I–125 for its effectiveness in treating ocular melanomas and effects to normal tissues.[1][23][24][25]

Iodine–125 has a half-life of 59.4 days and an average energy of 28.5 keV per gamma–ray. Palladium–103 has a half–life of 17 days and an average energy of 20.8 keV. Of the two radionuclides, I–125 is more commonly used to treat intraocular tumors.

I–125 offers a more homogeneous dose over the prescription point. However, the less homogeneous dose offered by Pd–103 provides an advantage to spare normal tissues. An investigation needs to be launches that examines the possible dosimetric advantages to using Pd–103 sources. Safety concerns, such as what protocols should be followed if a seed breaks open or becomes loose, must be recommended concluding this study.

A recommended study is to copy 3D plans with I–125 seeds in v6.3.1 and create a new treatment plan with Pd–103 seeds. By duplicating the treatment plan the only difference between the Pd–103 and I–125 plans are the radionuclide and the prescription dose; tumor dimensions and placement, plaque placement, implant time, and dose calculation parameters would remain identical for the first iteration of calculations.

In deciding the prescription dose to be associated with Pd-103 treatments, care should be given to the possible differences in radiobiological effectiveness (RBE) with respect to the two different sources. RBE measures the differences in how the living tissue responds to differences in the type of radiation and/or dose rate. While both I—125 and Pd—103 emit photons there is a difference in the energy of the emitted photons and the rate with which equivalent doses are delivered. The amount that the dose should be changed, if at all, is an active area of research that still has to be decided. In part, the move to standardize dose calculations is a step in that direction.

As an example, *Finger et al. 2009* reviews results of patients treated with Pd-103 treated to a prescription dose of 73.3 Gy.[24] His method of calculation assumes a point source in an infinite medium. In order to properly compare *Finger et al. 2009*'s data with other trials his dose calculations would have to be redone using more accurate line source calculation based on consensus date. Future studies will hopefully use consensus methods to calculate dose and allow research studies to compare "apples to apples."

The results of doses to the normal tissues as well doses at distances away from the inside of the sclera would be compared to each other to see if which isotope predicts lower doses to normal tissues while sufficiently irradiating the tumor.

For the second iteration of studies the implant time will be tweaked if the recommended minimium dose rate (0.60 Gy/hr) set by the American Brachytherapy Society is

not met.[26]

At OHSU an implant of 100 hours is assumed for I–125 seeds, but a different implant time may need to be adapted with Pd–103. *Gagne et al. 2012*[25] recommends adopting a shorter implant time if a higher dose rate is used, citing shorter implant times may correlate with more favorable outcomes than the standard 100 hours.

If Pd–103 offers a clear advantage over I–125 it is recommended that a discussion takes place between the physicist, ophthalmologist, and radiation oncologist on the benefits of treating with Pd–103 seeds. The data collected from this study will be the basis for the rationale to start using Pd–103 seeds at OHSU.

8.3. Modeling the eye with computed tomography or ultrasound images

Although there is little variation between the eye dimension from person to person, Plaque Simulator offers the capacity to model the dimensions of the eye through a manual entry or through calibrating computed tomography (CT) images.

A preliminary study has been created on modifying the eye size and eccentricity using standard eye dimensions in Plaque Simulator and has shown that normal tissue doses are effected by the size of the eye.

However, taking CT scans costs additional money to the patient and will give the patient potentially unnecessary radiation dose. It is recommended that patient records be examined for patients who also received a CT scan of their head and use the data from previous scans to model the eye size. The human eye stops growing and reaches its full size at puberty. Therefore we can expect the human eye to remain the same size, assuming the intraocular melanoma is small or medium sized and does not affect the size of the eye.

It is recommended that the original treatment plan is remade in 3D in v6.3.1 with the original seed strength from v5.3.9 and then copied. The copied treatment plan will have calibrated CT images and that model the patients eye and the original treatment plan will contain the default eye size of eccentricity of 1 and an eye diameter of 24 mm. The normal doses and doses at distances along the sclera will be compared.

If modeling the eye with a CT offers significant advantage then OHSU should consider modeling patient data with a CT scan. If the CT scan does not offer an advantage then OHSU can continue treating patients with the confidence that the default eye size is sufficient for obtaining normal tissue estimates.

8.4. Recalculating old treatment plans with a 3D method and investigating long–term toxicities with patients

The literature has cited the effect of radiation on visual ability. Many patients present at OHSU with a reduction or impairment of vision. The ability of a patient to retain their sight and eye remains an important quality of life consideration, especially for patients with longer life expectancies.

It is worthwhile to follow up with patients who have undergo eye plaque brachytherapy and to monitor how their vision has been affected. There are several factors for why a patient may be experiencing vision loss or reduction, but the relationship between radiation damage and normal tissue toxicity should be investigated.

Patients who elect to undergo this followup study should have their plans recreated in v6.3.1 using the 3D method described earlier. The seed strength input into v6.3.1 should be the same seed strength that was used in v5.3.9. Normal tissue estimates collected from 3D planning with v6.3.1 should be recorded. Although casual inference cannot be made from an observational study the occurrence of radiation–related side effects can be noted and correlated to the doses a critical structure received.

9. Conclusions

This thesis investigated the dosimetric and technical differences between v5.3.9 and v6.3.1 of Plaque Simulator. Twenty–eight patient plans originally created in v5.3.9 were recreated in v6.3.1. The doses to the prescription point, sclera, and tumor apex were recorded for each plan and the percent difference between the old and the new version were recorded and reported.

The percent difference between the prescription point between v5.3.9 and v6.3.1 was 0% for all (28 out of 28) cases. This is a trivial result as the treatment plan is created based on the dose to the prescription point. Any deviation from this value is indicative of human error or a change in treatment protocol.

Doses to the sclera are between 2–4% lower in v6.3.1 than v5.3.9. There were two cases with percent differences greater than 5% at –5.21 and –6.22%, respectively. The decrease in doses to the sclera between v5.3.9 and v6.3.1 are attributed to the change in the carrier factor correction data sets.

The carrier correction factor takes into account heterogeneities from the Silastic insert. Silastic ($Z_{eff} \sim 11$) has a higher atomic number than water ($Z_{eff} \sim 7.4$). A higher Z_{eff} gives a higher probability of the photoelectric effect, τ, as shown in Equation 9.1, where Z is the atomic number of the molecule the photon is interacting with and E is the energy of the photon.

$$\tau = \frac{Z^3}{E^3} \tag{9.1}$$

The heterogeneities of the Silastic insert is further exasperated by the short distances between the seed and the Silastic. Brachytherapy dosimetry at small distances is challenging and the methods for correcting for heterogeneities at short distances is still in development.

Plaque Simulator v6.3.1 uses carrier correction factor data from *Chiu Tsao et al. 1993*[10] which is based off the I–125 seed model 6711. The origin of the data set in v5.3.9 is unknown. The differences in the two data sets are largest (–7.80%) at $r =$ 0 mm which corresponds to the heterogeneity correction factor at the seed. The percent difference between the two data sets are –5.15% and –3.36% at $r = 1$ mm and $r = 2$ mm, respectively. The –5.15% and –3.36% also correspond to the outer and inner sclera

positions, respectively. Given these correction factor differences it is unsurprising that v6.3.1 calculates lower doses. Plaque Simulator v6.3.1's carrier correction factors, from *Chiu Tsao et al. 1993*, predicts larger heterogeneity corrections and greater attenuation of photons in the Silastic insert than v5.3.9's data set.

The data set from *Chiu Tsao et al. 1993* should be adopted until a more appropriate data set is found. Although *Chiu Tsao et al. 1993* is not for the IsoAid I–125 seed model used for OHSU its heterogeneity corrections, especially at $r = 0$ mm, is more realistic than v5.3.9 that does not predict any heterogeneity corrections at $r = 0$ mm.

There is also a change in the air correction factors used in v5.3.9 and v6.3.1. Plaque Simulator v5.3.9 uses a simple second–order equation found in *de la Zerda et al. 1996*[22]. The user cannot modify this equation or insert a data set in v5.3.9. Plaque Simulator v6.3.1 uses air correction data from *Thomson et al. 2008*[6] that is based off Monte Carlo data.

The air correction factor only affects anterior tumors and is turned off by default. The parameter, R, is the distance from the air interface to the point of measurement. The difference between the two data sets is greatest at $R = 3$ mm with a percent difference of 13.79% between *de la Zerda et al. 1996* and *Thomson et al. 2008*.

Although the differences in these data sets are significant for most distances from the air interface, the data set from *Thomson et al. 2008* should be adopted as it is based on Monte Carlo data. The air correction factor becomes negligible at distances greater than 15.0 mm from the air interface.

The doses to the tumor apex calculate no change in dose between v5.3.9 and v6.3.1 for 21% (6 out of 28) of cases. The cases that did see a change in dose, 68% (19 out of 28) of cases had a percent difference of less than 1% with the remaining three cases having percent differences of less than 1.5%.

It is recommended that v6.3.1 be accepted in clinical use after a few additional dosimetric tests are conducted. The decision of what correction data set should be used is a discussion that needs to happen between the physicist, radiation oncologist, and ophthalmologic surgeon with the understanding that the data set may change as new literature becomes available.

An additional study was launched establishing proof of concept of utilizing fundus images for three–dimensional (3D) planning. One–dimensional (1D) planning creates a treatment plan by prescribing a dose based on a single tumor dimension without regard to where the tumor is located within the eye. 3D planning attempts to orientate the tumor at its correct clock hour and anterior/posterior location within the eye. 1D treatment planning is capable of only calculating dose to the tumor apex; 3D treatment planning is able to calculate doses to normal tissues in addition to the apex of the tumor.

A proof of concept was launched to see how attempting to model the tumor at its correct clock hour and anterior/posterior position would affect the dose to the tumor prescription point, sclera, and tumor apex. Best guess estimations on the tumor positions were made based off the fundus image and the clockhours listed in the physician notes and ultrasound images. The recreated plans from the study comparing v5.3.9 and v6.3.1 were duplicated and a new 3D plan was created using v6.3.1.

As with the study comparing v5.3.9 to v6.3.1, there was a 0% difference to the prescription point for all (28 out of 28) cases. This result is a double check that there is no change to the prescription point and dose between the two cases.

Doses between 1D and 3D planning were minimal. The study revealed 75% (21 out of 28) cases had no change to the sclera between 1D and 3D planning. Of the cases where there changes in the dose between 1D and 3D planning methods the change to dose in the sclera was no greater than 0.06%.

The doses to the tumor apex remained unchanged for 93% (26 out of 28) cases between 1D and 3D planning methods. The cases that saw a change in dose to the tumor apex had percent differences of 0.1% and 0.01%, respectively.

Proof of concept that 3D planning can be implemented without major changes between 1D and 3D calculation methods to the tumor has been established. Although the tumor positions in the 3D plans are best guesses and should be taken with a grain of salt, it is important to note the diversity of positions within this study represent the variety of tumor positions within patients.

In other words, it does not hurt the current treatment planning process to plan cases by moving the tumor to different locations in the eye. The largest percent difference between 1D and 3D methods for the current cohort was no greater than 0.1%. The quality of care to the patient is not being harmed by creating treatment plans using 3D methods.

The advantages of 3D methods, calculating accurate normal tissues doses, outweighs the potential disadvantages of 3D planning. To minimize the uncertainty in tumor position a calibrated fundus image can help guide the physicist in positioning the tumor. In cases where the tumor is anterior and no fundus image is available the ophthalmologist may assist in placing the tumor. It is strongly recommended that OHSU moves toward 3D planning methods to better calculate doses to normal tissues to patients electing to undergo eye plaque brachytherapy.

Future studies may increase the quality of care for eye plaque brachytherapy cases at OHSU. In particular a study examining the performance of Plaque Simulator v6.3.1 with different tumor apices for each COMS plaque and study investigating the implementation of Palladium–103 sources in lieu of I–125. The increased dosimetric and imaging

capabilities of v6.3.1 will allow the eye plaque brachytherapy program at OHSU to create more sophisticated treatment plans that give more accurate normal tissues doses to the patient.

Bibliography

[1] S.-T. Chiu-Tsao, M. A. Astrahan, P. T. Finger, D. S. Followill, A. S. Meigooni, C. S. Melhus, F. Mourtada, M. E. Napolitano, R. Nath, M. J. Rivard, *et al.*, "Dosimetry of 125i and 103pd coms eye plaques for intraocular tumors: Report of task group 129 by the aapm and abs," *Medical physics*, vol. 39, no. 10, pp. 6161–6184, 2012.

[2] A. Singh and B. Hayden, *Ophthalmic Ultrasonography*. ClinicalKey 2012, Elsevier/Saunders, 2011.

[3] C. O. M. S. Group *et al.*, "Design and methods of a clinical trial for a rare condition: the collaborative ocular melanoma study: Coms report no. 3," *Controlled Clinical Trials*, vol. 14, no. 5, pp. 362–391, 1993.

[4] C. O. M. S. Group *et al.*, "The collaborative ocular melanoma study (coms) randomized trial of pre-enucleation radiation of large choroidal melanoma iii: local complications and observations following enucleation coms report no. 11," *American journal of ophthalmology*, vol. 126, no. 3, pp. 362–372, 1998.

[5] C. O. M. S. Group *et al.*, "The coms randomized trial of iodine 125 brachytherapy for choroidal melanoma: V. twelve-year mortality rates and prognostic factors: Coms report no. 28.," *Archives of ophthalmology (Chicago, Ill.: 1960)*, vol. 124, no. 12, p. 1684, 2006.

[6] R. Thomson, R. Taylor, and D. Rogers, "Monte carlo dosimetry for i125 and pd103 eye plaque brachytherapy," *Medical physics*, vol. 35, no. 12, pp. 5530–5543, 2008.

[7] R. Nath, L. Anderson, G. Luxton, *et al.*, "Dosimetry of interstitial brachytherapy sources. recommendations of the american association of physicists in medicine. tg-43," *Med Phys*, vol. 22, pp. 209–234, 1995.

[8] M. J. Rivard, B. M. Coursey, L. A. DeWerd, W. F. Hanson, M. S. Huq, G. S. Ibbott, M. G. Mitch, R. Nath, and J. F. Williamson, "Update of aapm task group no. 43 report: A revised aapm protocol for brachytherapy dose calculations," *Medical physics*, vol. 31, no. 3, pp. 633–674, 2004.

[9] M. J. Rivard, W. M. Butler, L. A. DeWerd, M. S. Huq, G. S. Ibbott, A. S. Meigooni, C. S. Melhus, M. G. Mitch, R. Nath, and J. F. Williamson, "Supplement to the 2004 update of the aapm task group no. 43 report," *Medical physics*, vol. 34, no. 6, pp. 2187–2205, 2007.

[10] S.-T. Chiu-Tsao, L. L. Anderson, K. O'Brien, L. Stabile, and J. C. Liu, "Dosimetry for 125i seed (model 6711) in eye plaques," *Medical physics*, vol. 20, no. 2, pp. 383–389, 1993.

[11] M. A. Astrahan, G. Luxton, Q. Pu, and Z. Petrovich, "Conformal episcleral plaque therapy," *International Journal of Radiation Oncology* Biology* Physics*, vol. 39, no. 2, pp. 505–519, 1997.

[12] G. Luxton, M. A. Astrahan, P. E. Liggett, D. L. Neblett, D. M. Cohen, and Z. Petrovich, "Dosimetric calculations and measurements of gold plaque ophthalmic irradiators using iridium-192 and iodine-125 seeds," *International Journal of Radiation Oncology* Biology* Physics*, vol. 15, no. 1, pp. 167–176, 1988.

[13] C. S. Melhus and M. J. Rivard, "Coms eye plaque brachytherapy dosimetry simulations for 103pd, 125i, and 131cs.," *Medical physics*, vol. 35, no. 7, pp. 3364–3371, 2008.

[14] R. Thomson and D. Rogers, "Monte carlo dosimetry for i125 and p103d eye plaque brachytherapy with various seed models," *Medical physics*, vol. 37, no. 1, pp. 368–376, 2010.

[15] S.-T. Chiu-Tsao, K. O'Brien, R. Sanna, H.-S. Tsao, C. Vialotti, Y.-S. Chang, M. Rotman, and S. Packer, "Monte carlo dosimetry for 125i and 60co in eye plaque therapy," *Medical physics*, vol. 13, no. 5, pp. 678–682, 1986.

[16] H. Zhang, D. Martin, S.-T. Chiu-Tsao, A. Meigooni, and B. R. Thomadsen, "A comprehensive dosimetric comparison between 131 cs and 125 i brachytherapy sources for coms eye plaque implant," *Brachytherapy*, vol. 9, no. 4, pp. 362–372, 2010.

[17] J. Dudee, "Anterior Segment and Fundus Photography." `http://emedicine.medscape.com/article/1228681-overview#a11`, 2015. [Online; accessed 03-May-2016].

[18] R. G. Waldron, "B-Scan Ocular Ultrasound." `http://emedicine.medscape.com/article/1228865-overview#a1`, 2016. [Online; accessed 03-May-2016].

[19] M. J. Rivard, S.-T. Chiu-Tsao, P. T. Finger, A. S. Meigooni, C. S. Melhus, F. Mourtada, M. E. Napolitano, D. Rogers, R. M. Thomson, and R. Nath, "Comparison of dose calculation methods for brachytherapy of intraocular tumors," *Medical physics*, vol. 38, no. 1, pp. 306–316, 2011.

[20] T. D. Solberg, J. J. DeMarco, G. Hugo, and R. E. Wallace, "Dosimetric parameters of three new solid core i-125 brachytherapy sources," *Journal of Applied Clinical Medical Physics*, vol. 3, no. 2, pp. 119–134, 2002.

[21] A. S. Meigooni, J. L. Hayes, H. Zhang, and K. Sowards, "Experimental and theoretical determination of dosimetric characteristics of isoaid advantage™ 125i brachytherapy source," *Medical physics*, vol. 29, no. 9, pp. 2152–2158, 2002.

[22] A. de La Zerda, S.-T. Chiu-Tsao, J. Lin, L. L. Boulay, I. Kanna, J. H. Kim, and H.-S. Tsao, "125i eye plaque dose distribution including penumbra characteristics," *Medical physics*, vol. 23, no. 3, pp. 407–418, 1996.

[23] P. T. Finger, A. Berson, T. Ng, and A. Szechter, "Palladium-103 plaque radiotherapy for choroidal melanoma: an 11-year study," *International Journal of Radiation Oncology* Biology* Physics*, vol. 54, no. 5, pp. 1438–1445, 2002.

[24] P. T. Finger, K. J. Chin, G. Duvall, P.-. for Choroidal Melanoma Study Group, *et al.*, "Palladium-103 ophthalmic plaque radiation therapy for choroidal melanoma: 400 treated patients," *Ophthalmology*, vol. 116, no. 4, pp. 790–796, 2009.

[25] N. L. Gagne, K. L. Leonard, and M. J. Rivard, "Radiobiology for eye plaque brachytherapy and evaluation of implant duration and radionuclide choice using an objective functiona)," *Medical physics*, vol. 39, no. 6, pp. 3332–3342, 2012.

[26] T. Force, A.-O. Committee, *et al.*, "The american brachytherapy society consensus guidelines for plaque brachytherapy of uveal melanoma and retinoblastoma," *Brachytherapy*, vol. 13, no. 1, pp. 1–14, 2014.